TOPICAL REVIEW

Inorganic ligand capped quantum dot light-emitting diodes: status and perspective

To cite this article: Tianxu Zhang *et al* 2025 *Nanotechnology* **36** 102001

IOP Publishing Nanotechnology

Nanotechnology **36** (2025) 102001 (19pp) https://doi.org/10.1088/1361-6528/ada2f1

Topical Review

Inorganic ligand capped quantum dot light-emitting diodes: status and perspective

Tianxu Zhang[1], **Xuan Yang**[1], **Bin Xie**[2,*] **and Xiaobing Luo**[1,*]

[1] School of Energy and Power Engineering, Huazhong University of Science and Technology, Wuhan 430074, People's Republic of China
[2] School of Mechanical Science and Engineering, Huazhong University of Science and Technology, Wuhan 430074, People's Republic of China

E-mail: binxie@hust.edu.cn and luoxb@hust.edu.cn

Received 5 June 2024, revised 18 August 2024
Accepted for publication 24 December 2024
Published 6 January 2025

Abstract

Quantum dots (QDs) have shown great application potential in a variety of optoelectronic devices due to their unique optoelectronic properties, especially playing a key role in the development of quantum dot light-emitting diodes (QLEDs). Inorganic ligands, including metal or non-metal chalcogenides, oxoanions, halides, and metal cations, play crucial roles in the synthesis, stabilization, and functionalization of QDs. Compared to long-chain organic ligands, inorganic ligands are shorter and possess higher electron mobility, which facilitates their application in high-performance QLEDs. This review explores the mechanisms of ligand exchange, classifies the types of inorganic ligands, and discusses their impact on the properties of QDs. Special attention is given to the latest research developments in inorganic ligand QDs for LEDs and their prospective applications in optoelectronics. This review highlights the versatility and efficacy of inorganic ligands, showcasing their potential to revolutionize QLED technology for future high-resolution displays and efficient optoelectronic devices.

Keywords: quantum dots, inorganic ligands, QD-LED, surface passivation

1. Introduction

Quantum dots (QDs) are nanocrystals (NCs) with a size between 1 and 10 nm, with superior electronic and optical properties due to their unique quantum confinement and surface effects [1–4]. The properties of these nanoparticles are not only affected by their composition and structure, but also depend on the size and shape at the nanoscale, providing wide and tunable band gaps, narrow emission peaks, high luminescence quantum yields, and good optics stability [1, 5–8]. This advanced material has been widely used in light sources [9–11], information display technology (such as full-color displays and virtual reality devices) [12–15], solar cells [16–19] and biological imaging [20–23]. As synthesis methods advance and a deeper understanding of their properties emerges, QDs are becoming the center of cutting-edge research across multiple scientific and engineering disciplines, driving the continuous development of new technologies and applications.

The surface ligands of QDs play a crucial role in their synthesis, stability, and functionalization. Ligands can passivate unsaturated bonds on the surface of QDs and reduce the generation of non-radiative recombination centers (i.e. defects) [24, 25], thus improving the optoelectronic properties and stability of QDs. In colloidal NC chemistry, ligands not only affect the

* Authors to whom any correspondence should be addressed.

nucleation and growth process of QDs, but also regulate their dispersion and stability in different solvents by controlling the charge balance and polarity of the QD surface [26–29]. In addition, ligands can further change the optical and electronic properties of QDs by adjusting the energy positions at the edges of the conduction band and valence band [30–33].

The type and structure of the ligands are critical to the application of QDs. Long-chain hydrophobic ligands enhance the stability of QDs in nonpolar organic solvents, thereby improving photoluminescence quantum yield (PLQY) [34, 35]. However, these bulky ligands are usually insulating and non-functional [26, 36, 37], which limits their applicability in fields requiring efficient charge transport, such as electroluminescent quantum dot light-emitting diode (QLED). In contrast, inorganic ligands, which are typically shorter, exhibit higher electron mobility compared to their organic counterparts. Their compact size and high conductivity improve electron transport and biocompatibility [28, 38–40], making them essential for the development of more efficient optoelectronic devices and advanced biomedical applications.

In this review, we first introduce the mechanism of the passivation process of inorganic ligands in detail. Then, various inorganic ligands currently studied are classified and summarized, emphasizing their improvement in the properties of QDs such as luminescence, electron transport, and stability. Finally, we focus on the latest research progress in the application of inorganic ligand QDs (ILQDs) in LEDs, and prospect their future applications in the field of optoelectronics based on existing shortcomings and challenges.

In this review, we begin by providing a detailed introduction to the passivation mechanisms of inorganic ligands. We then classify and summarize various inorganic ligands currently under study, highlighting their contributions to enhancing the properties of QDs, including luminescence, electron transport, and stability. Following this, we explore the latest advancements in the application of ILQDs in LEDs, with a particular focus on device architecture, performance parameters, and how ILQDs contribute to improved device efficiency. Finally, we conclude by summarizing the key findings, addressing the challenges and limitations of current ILQD-based QLEDs, and offering insights into potential solutions and future research directions.

2. Inorganic ligand exchange process of inorganic ligand-terminated colloidal QDs

The synthesis technology of semiconductor material QD is mainly based on the high-temperature organic phase route [9, 41, 42]. Through this method, the surfaces of QDs are capped with organic ligands containing long carbon chains (such as oleic acid (OA), oleylamine (OAm), trioctylphosphine (TOP), etc), [43, 44] allowing these highly crystalline, monodispersed QDs to be stably dispersed in non-polar solvents (such as hexane, toluene, etc) [8, 9, 45].

Although organic ligands play an important role in the synthesis of QDs, their long carbon chain structures limit their applications in those fields that require stronger hydrophilicity or specific surface functionality, as mentioned above. Researchers have developed a variety of methods to remove or replace organic ligands on the surface, including thermal treatment [46–48], chemical etching [49–51], UV/Ozone [52–54] and plasma [55–57], etc. However, these techniques are often accompanied by some shortcomings, such as the possible damage to the structure of QDs, partial oxidation of QDs, or the incurrence of surface defects [58, 59].

Relatively speaking, solution-phase inorganic ligand replacement technology provides an effective alternative due to its mild operating conditions and small impact on QDs [60]. This method achieves replacement with organic ligands by introducing inorganic ligands into the solution, which not only retains the original structure and optoelectronic properties of QDs, but also meets the surface functional requirements of specific applications. Furthermore, the advancement of this technology enriches the approaches for surface modification of QDs and broadens their potential for widespread use in scientific research and technological applications.

Ligand exchange in the solution phase can facilitate the transfer of QDs between polar and nonpolar solvents. Taking the surface regulation of II–VI core–shell QDs with indium nitrate ($In(NO_3)_3$) as an example, solutions of red-emitting CdSe/ZnS QDs, green-emitting CdSe/CdZnSeS/ZnS QDs, and blue-emitting CdZnS/ZnS QDs in hexane were added to a dimethylformamide (DMF) solution containing indium nitrate. This resulted in a distinct phase separation [61]. After vigorous stirring, the transfer of QDs from the nonpolar hexane phase to the polar DMF phase was observed (figure 1(a)). In the DMF phase, indium ions (In^{3+}) replaced the original organic ligand OA on the surface of the QDs, while nitrate ions (NO_3^-) serve as counter ions to form a diffusion around QDs (figure 1(b)). The ion layer maintains the charge neutrality of the entire system. The electrostatic interaction between nitrate ions and indium ions not only ensured high dispersion of the QDs but also enhanced their stability in the polar solvent. Moreover, further washing and purification with a less polar anti-solvent, such as toluene, effectively removed unreacted free indium ions, nitrate ions, and other impurities, furtherly enhancing the quality and purity of the QDs. The obtained indium-ion-modified QDs could be redispersed in fresh solvents as required.

When delving into the interaction between QDs and inorganic ligands, the covalent bond classification theory provides an extremely effective analytical framework (figure 2). This theory divides ligands into three major categories: ① L-type ligands serve as two-electron donors, usually Lewis bases. They form coordination bonds with metal ions by providing lone pairs of electrons, such as amines (R-NH_2), phosphine (R_3-P) and its oxide (R_3-PO). ② X-type ligands, which act as one-electron donors, can repair defects on the surface of NCs by filling vacancies, with typical examples including halide ions (Cl^-, Br^-), carboxylate (R-COO^-) and thiolate (R-S^-). ③ Z-type ligands serve as two-electron acceptors, usually Lewis acids, which can accept electron pairs and are used for passivation or stabilize the surface of QD, such as certain metal

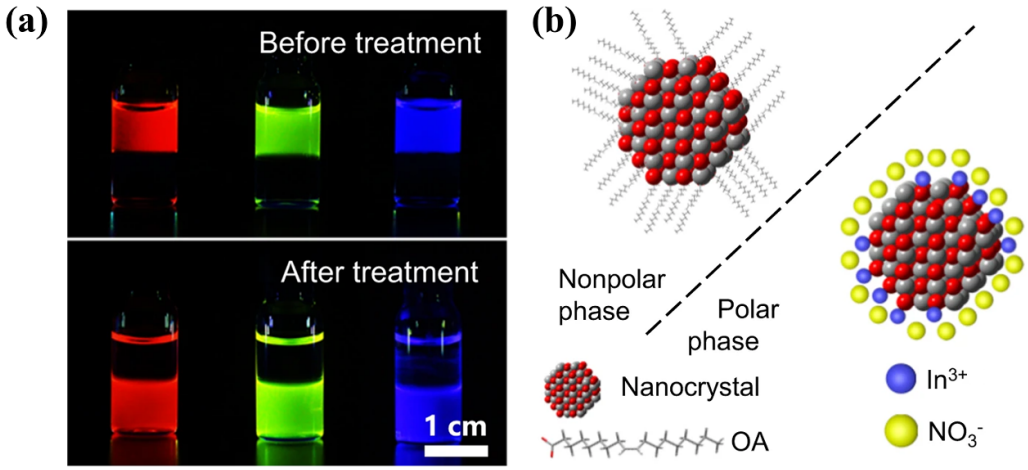

Figure 1. (a) Optical images of red-emitting CdSe/ZnS QDs, green-emitting CdSe/CdZnSeS/ZnS QDs and blue-emitting CdZnS/ZnS QDs before and after treatment with $In(NO_3)_3$ under UV light. The solvents of the upper and lower layers were hexane and DMF, respectively. (b) Stable structures of organic ligand QD (left) and inorganic ligand QD (right) in non-polar and polar solvents, respectively. Reproduced from [61]. CC BY 4.0.

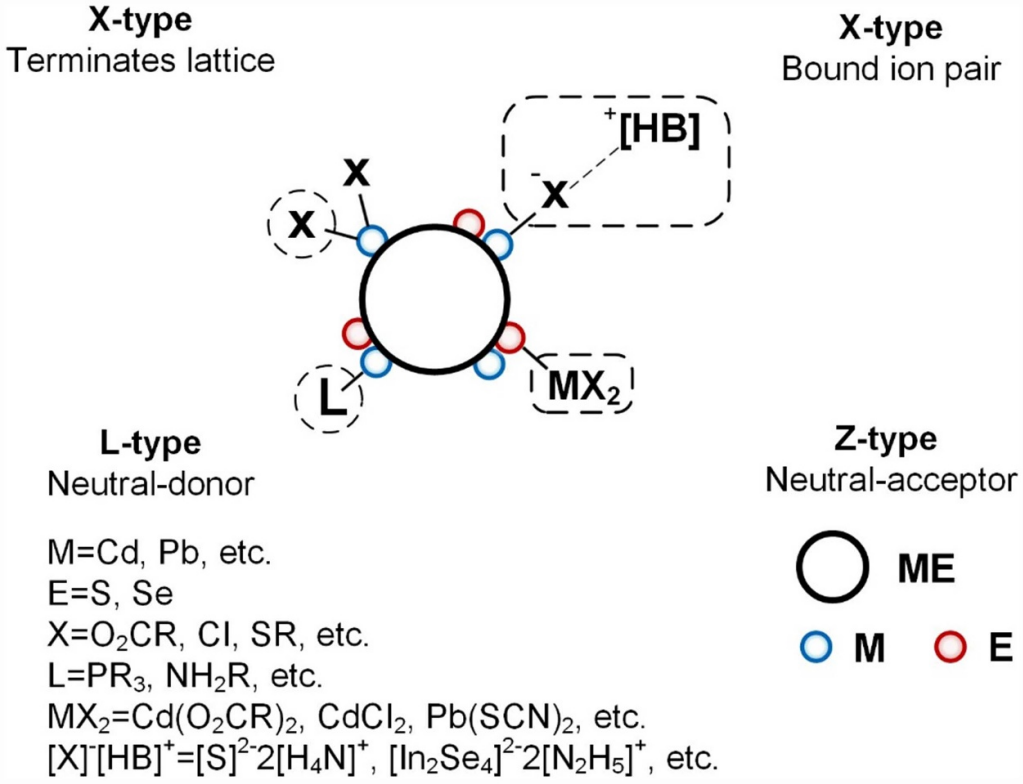

Figure 2. Nanocrystal ligand binding motifs according to the covalent bond classification method. Reprinted (adapted) with permission from [35]. Copyright (2013) American Chemical Society.

salts ($CdCl_2$, $ZnCl_2$) [62–65]. This classification simplifies the understanding of ligand behavior, particularly in dealing with complex inorganic-organic interfaces.

In the synthesis process of QDs, long-chain organic ligands usually appear as X-type ligands, mainly including oleate and other fatty acid derivatives, which cap QDs by forming coordination bonds with excess metal cations on the surface to prevent further growth and aggregation. At this time, this binding motif of QDs can be expressed as $NC(MX_n)$ according to the unified representation method of NCs [66]. Inorganic ligands can be used as X-type ligands to combine with surface metal or non-metal atoms by providing single electrons, or they can be used as Z-type ligands to accept electron pairs and react with Lewis basic sites of nanoparticles. The exchange reaction of X-type organic ligand and X-type inorganic ligand can be written as: [65]

$$NC(MX_2) + 2HX' \rightleftharpoons NC(MX_2') + 2HX. \quad (1)$$

For example, X = $RCOO^-$, RS^-; X' = CI^-, SCN^-.

Generally, the reaction of X-type organic ligands with Z-type inorganic ligands can cause QDs to be transferred from non-polar solvents to polar solvents (figure 1(b)). Its exchange reaction can be written as: [50]

$$NC(MX_2) + Z \rightleftharpoons NC(MX)^+ + (ZX)^-. \quad (2)$$

For example, X = $RCOO^-$, RS^-; Z = $CdCl_2$, $ZnCl_2$.

3. Diversity of inorganic ligands and the impact on QDs

A revolutionary development in QD technology is the introduction of solution-phase inorganic ligand exchange, a concept first proposed by Talapin and his team in 2009 [40]. In their pioneering work, traditional natural organic ligands were replaced by inorganic species—molecular metal chalcogenide complexes (MCCs). The obtained QD NCs can be dispersed in polar solvents and transformed into crystalline or amorphous states after heat treatment for the use in semiconductor devices such as transistors. Since this breakthrough study by the Talapin's team, as many as 81 different inorganic ligands have been developed, which can be classified into five categories: MCCs, metal-free chalcogenide complexes (MFC), oxoanions, halides and metal halides, and metal cations.

3.1. Metal chalcogenide complex

Talapin and colleagues were the pioneers in using MCCs, such as $Sn_2S_6^-$, $In_2Se_4^{2-}$, In_2Te_3, Ga_2Se_3, $CuInSe_3$, ZnTe, $HgSe_2^{2-}$, Sb_2Se_3 as capping agents for QD NCs (figure 3(a)) [40]. The synthesis of these MCC ligands typically involves dissolving main group or transition metal chalcogenides in hydrazine, forming soluble anions, for example, $Sn_2S_6^-$ (figure 3(b)). Hydrazine ($N_2H_5^+$) serves as the cation, not interacting directly with the NCs but forming a diffuse ionic layer around them to maintain charge neutrality. This biphasic ligand exchange process allows NCs to transition smoothly from nonpolar solvents like toluene to polar solvents such as formamide or dimethyl sulfoxide (DMSO), without compromising their optical properties. The distinctive feature of MCC is that it can transform from an insulator phase to a semiconductor phase through heat treatment without changing the chemical properties of QDs, providing a new idea for manufacturing semiconductor materials [40, 67]. For instance, upon heating at 180 °C, $Sn_2S_6^{4-}$ decomposes cleanly into SnS_2 and gases, leaving no carbon-containing impurities: $(N_2H_5)_4Sn_2S_6 \rightarrow SnS_2 + 4N_2H_4 + 2H_2S$ [68]. This reaction results in the formation of high-purity, electronic-grade SnS_2 semiconductors, ideal for use in semiconductor thin-film devices. Recent studies have further revealed the properties of MCC ligands: these inorganic ligands spontaneously dissociate on the QD surface and form an amorphous matrix around the core. This passivation layer builds a bridge for electron transmission between QDs, thereby improving the electron mobility of inorganic QD devices [69].

The diversity of MCC plays a pivotal role in modulating the properties of inorganic colloidal QDs and their resultant films, impacting key characteristics such as electrical conductivity, magnetic susceptibility, and electrocatalytic activity [73]. For instance, the incorporation of metal ions such as Cd^{2+}, Ca^{2+}, and In^{3+} can fundamentally alter the surface charge of QDs, switching it from negative to positive. Moreover, the introduction of K^+ ions into MCC can transform the conductivity characteristics of MCC-terminated CdTe QDs from p-type to n-type. This modification not only adjusts the charge transport properties but also enhances the photoluminescence attributes of the QDs. Mn^{2+} connects the S^{2-} terminated CdSe QDs by forming an S–Mn–S type bond bridge, imparting magnetic properties to the otherwise non-magnetic CdSe QDs. The presence of Pt^{2+} ions is particularly crucial in dictating the electrocatalytic behavior of semiconductor QD solids. These ions facilitate the fine-tuning of electrochemical reactions at the nanoscale, enhancing the performance of QD-based catalysts [73]. In particular, MCC ligands can form stronger binding with chalcogenide-based QDs due to the strong affinity between metal elements and chalcogenides [40, 74–76].

Furthermore, MCCs based on main group metals, such as $Na_4Sn_2S_6$, $Na_4Sn_2Se_6$, $(NH_4)_4Sn_2S_6$, K_4SnTe_4, $(NH_4)_3AsS_3$ and Na_3AsS_3 can effectively passivate semiconductor QDs like CdSe and PbS (figure 3(c)), significantly enhancing the charge transport properties of films and suspensions while preserving quantum effects and exciton absorption peaks [70, 75].

MCC ligands bring the NCs into closer proximity, reducing the interparticle distance to 0.3 nm (approximately 1/5 that of organic ligands)[77], thereby enhancing wave function overlap and promoting strong electronic coupling that favors metallic behavior. Furthermore, these ligands impart substantial charges to the NCs, balancing electrostatic and van der Waals forces to promote the formation of ordered superstructures in polar solvents. In the latest research conducted by Talapin's team, they used multivalent salts to control micron-scale supercrystalline assembly of inorganic NCs [77]. These supercrystals are composed of $Sn_2S_6^{4-}$ and $Sn_2Se_6^{4-}$ terminated metal NCs (metals such as Au, Pt and Ni or semiconductors such as PbS and PbSe), which exhibit extremely high electronic coupling capabilities and provide a promising platform for the fabrication of QD thin film transistors. Additionally, MCCs include less common transition metal-based thiometallates such as PtS_{15}^{2-}, CoS_9^{2-}, NiS_6^{2-}, $Fe_2S_{12}^{2-}$, MoS_4^{2-}, WS_4^{2-} [40, 78, 79], etc, which have also received research attention in recent years. The properties of these compounds are similar to traditional MCCs and exhibit similar principles, nonetheless, upon heat treatment, these thiometallates can form nanoscale transition metal or transition metal sulfide structures on the surface of QDs, imparting catalytic activity to the QDs.

However, MCC also exhibit certain notable drawbacks. For instance, QDs capped with MCC are typically dispersible only in highly polar solvents. Addressing this limitation, researchers have devised innovative solutions such as the coordination of MCC-capped QDs with macrocyclic ethers, facilitating the solubilization of inorganically capped NCs in

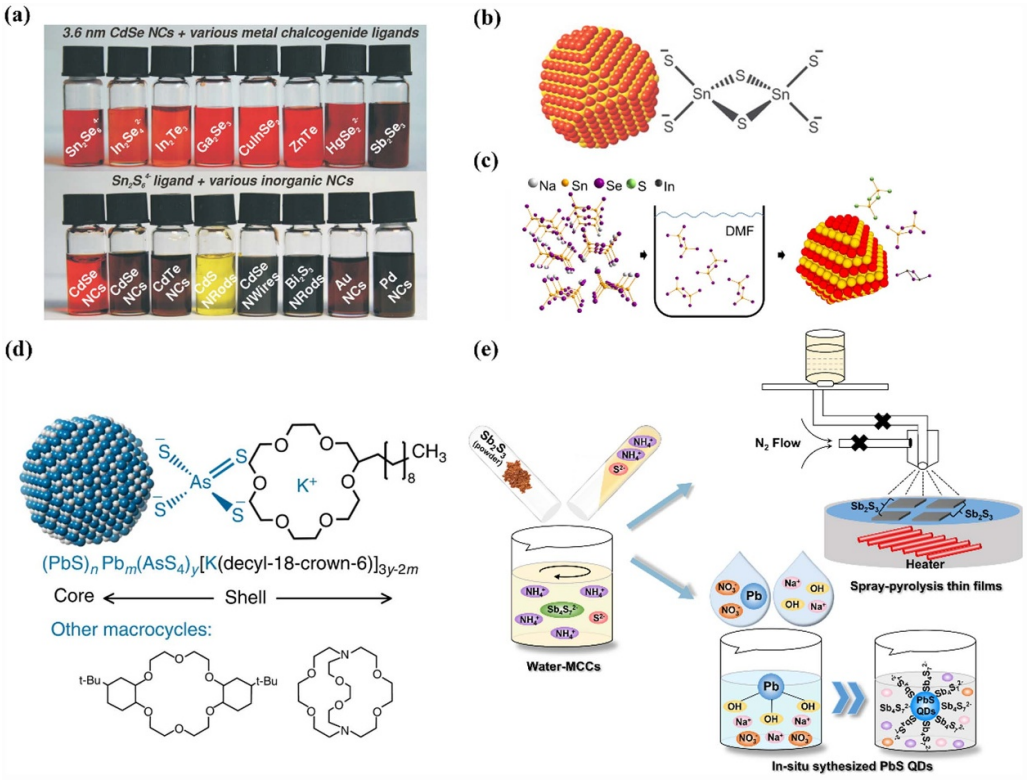

Figure 3. (a) Stable colloidal solutions of CdSe QDs capped by various metal chalcogenide complexes. (b) CdSe QDs using $Sn_2S_6^{-}$ as ligand. From [40]. Reprinted with permission from AAAS. (c) Schematic diagram of the combination of main group metal sulfide ligands and CdSe QDs. Reprinted with permission from [70]. Copyright (2018) American Chemical Society. (d) Schematic diagram of the complexation of MCC-terminated QDs with crown ethers or cryptands. Reproduced from [71]. CC BY 4.0. (e) Schematic diagram of the water-based solution MCC synthesis method and its application in the preparation of QD films and *in-situ* synthesis of QDs. Reprinted with permission from [72]. Copyright (2015) American Chemical Society.

solvents of varying polarity (figure 3(d)) [71]. Moreover, conventional methods for synthesizing MCC often require the use of hydrazine, a toxic and explosive chemical, which restricts its broader application. In response, a novel aqueous based synthesis method for MCC has been developed [72]. This method, which avoids the use of hydrazine, presents an environmentally benign and safer alternative, significantly broadening the prospects for MCC applications in the solution processing of inorganic semiconductors (figure 3(e)).

3.2. Metal-free chalcogenide complex

In an innovative work by Nag *et al* in 2011 [80], metal-free chalcogenides (such as chalcogenides and hydrogen chalcogenides S^{2-}, Se^{2-}, Te^{2-}, HS^{-}, HSe^{-} and HTe, non-metal sulfides complex TeS_3^{2-} etc) was used for the first time in the coordination of NCs as a substance opposite to metal chalcogenide (figure 4(a)). Metal-free chalcogenide complexes (MFC) usually do not contain metal elements, are low-cost and environmentally friendly. In addition, it also has the advantages of simple structure and small size (figure 4(c)), and can be widely used in mass production.

However, some researchers have identified persistent challenges with QDs surfaces after replacing organic ligands with Se^{2-} or S^{2-}, noting the presence of high-density trap states and weak hole transport capabilities. These deficiencies can be ameliorated by employing $PbCl_2$ to reduce the density of trap states and achieve n-type doping [81]. Moreover, MFCs exhibit varying degrees of affinity and application limitations. For instance, in the case of CdSe/ZnS QDs, S^{2-} demonstrates a higher affinity compared to many MCCs. Nonetheless, MCCs perform more effectively in conjunction with Pb chalcogenide QDs, whereas S^{2-} typically fails to successfully cap such structures [80]. Furthermore, compared to MCC-capped QDs, free chalcogenide ions, such as S^{2-}, are more susceptible to oxidative degradation in environmental conditions [26]. It has been observed that superior stability compared to MCC-capped QDs can only be achieved by preparing and storing the QDs in a glove box environment.

3.3. Oxoanions

Research on oxoanions ligands can be traced back to the end of the 20th century, when researchers began to explore the role of inorganic anions such as SO_4^{2-} and PO_4^{-} in improving the optical properties of QDs [82]. These substances show great potential in QD surface engineering due to their excellent electron storage capabilities and structural stability.

In 2014, Huang *et al* reported that using inorganic oxoanions (such as VO_4^{3-}, MoO_4^{2-}, WO_4^{2-}, PO_4^{3-} and MoO_4^{2-}) as ligands (figure 5(a)) can achieve stronger binding to oxide NCs (such as Fe_2O_3, ZnO and TiO_2), [83]

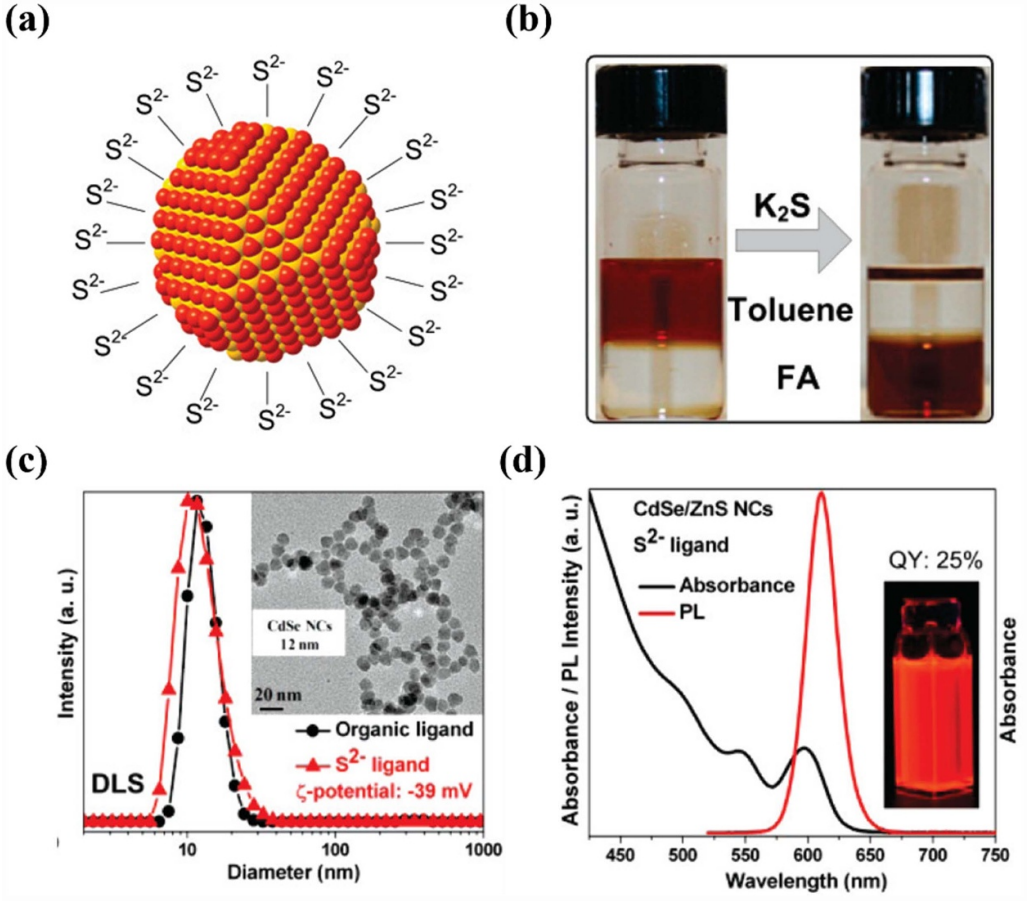

Figure 4. (a) Schematic diagram of CdSe QDs using S^{2-} to complete ligand exchange (b) Phase transfer of CdSe QD colloidal solution from toluene to formamide (FA) after using S^{2-} ligand to exchange organic ligands (c) Size distribution of organic ligands and S^{2-} ion-terminated CdSe QDs (d) Absorption and PL spectra of S^{2-} ligand CdSe/ZnS core/shell QDs; the inset shows the luminescence of the QD colloidal solution under 365 nm ultraviolet light irradiation. Reprinted with permission from [80]. Copyright (2011) American Chemical Society.

whereas previously studied chalcogenide ligands prefer to bind to metal sulfide QDs (e.g. cadmium selenide). This phenomenon can be explained by the hard–soft acid–base principle. Oxoanions usually belong to hard Lewis bases, and hard bases tend to form stable complexes with hard acids, so oxoanions can achieve more stable combinations with QDs with hard Lewis acidic sites. In addition, this study also shows that polyoxometalates such as $[PMo_{12}O_{40}]^{3-}$, $[P_2W_{18}O_{62}]^{6-}$, $[Mo_{126}^{VI}Mo_{28}^{V}O_{462}H_{14}(H_2O)_{54}(H_2PO_2)_7]^{21-}$ and other complex oxoanions can not only react with the surface of QDs as ligands, but also make them electrocatalytically active when combined with specific QDs.

Although the application of oxoanions ligands in QDs research has made remarkable achievements, there are many ions with weak nucleophilicity and weak binding force, such as NO^{3-}, PO_4^{3-}, SO_4^{2-} and ClO^{4-} [84], these ions are usually difficult to form stable coordination complexes due to their large charge density and small polarizability [85]. Studies have shown that hydrogenated forms of ions, such as $H_2PO_4^-$ and HSO_4^-, show better results than their normal forms PO_4^{3-} and SO_4^{2-} [84, 86]. Furthermore, using counterions with corresponding salts that have the ability to generate H^+ is also more effective in some cases. For example, in ammonium salt (CO_3^{2-}, $S_2O_3^{2-}$, SO_3^{2-}, NO_3^-) ionic liquids, they are more effective than other simple counterions [84, 87, 88]. This is due to the introduction of additional H^+, which increases the polarity and nucleophilicity of the ions, thereby improving their activity in coordination reactions.

3.4. Halides and metal halides

Pseudohalide ammonium thiocyanate (NH_4SCN) was first introduced into QD ligand engineering in 2011 as a new environmentally friendly short inorganic ligand (figure 6(a)) [89]. Its unique vibrational spectrum and high oscillation intensity provide unprecedented understanding for studying the chemical and electronic properties of QDs NC surfaces. After that, researchers conducted extensive research on halides and metal halides [90–96]. Niu *et al* reported the use of inorganic halogen ligands: I^-, Br^-, Cl^- to cap CdSe and PbS QDs, and the treated QDs were successfully subjected to electrophoretic deposition for the first time, significantly improving QDs film photocurrent [90]. Dirin *et al* proposed a general method for surface functionalization of QDs with metal halides (AMX_n

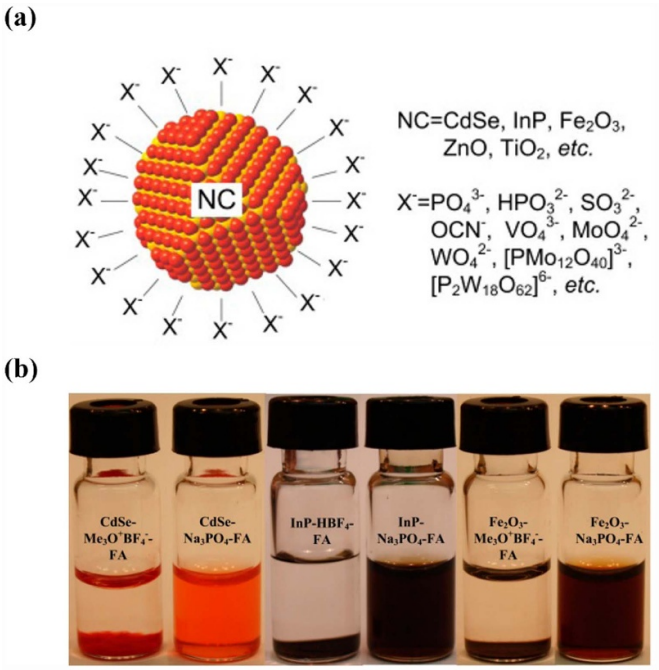

Figure 5. (a) Schematic diagram of the NCs structure of oxoanions ligands (b) Colloidal solution of CdSe, InP and Fe_2O_3 in FA treated by Me_3OBF_4 and then added with Na_3PO_4. Reprinted with permission from [83]. Copyright (2014) American Chemical Society.

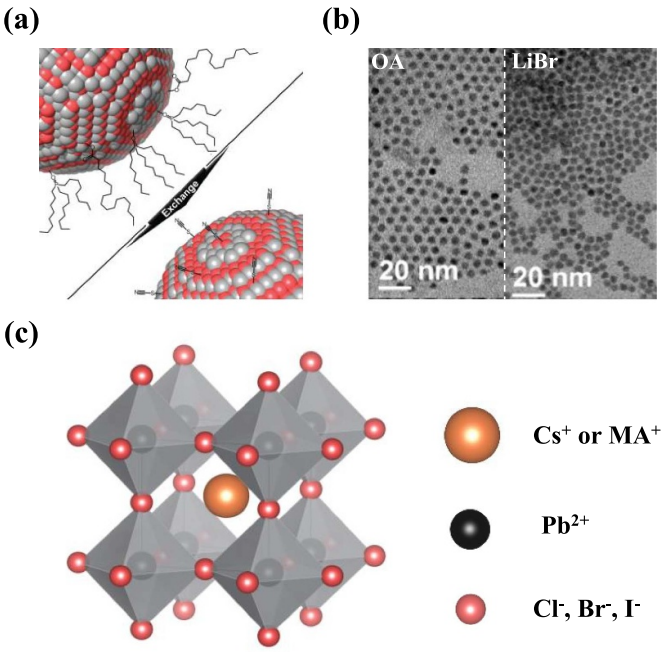

Figure 6. (a) Schematic diagram of the exchange of SCN^- with long-chain organic ligands. Reprinted with permission from [89]. Copyright (2011) American Chemical Society. (b) TEM images of PbSe QDs using oleic acid (left) and lithium bromide (right) as ligands. Reprinted with permission from [102]. Copyright (2017) American Chemical Society. (c) Typical halide perovskite QD structure. Adapted from [103] with permission from the Royal Society of Chemistry.

or MX_n, where M = Pb, Cd, Zn, In, Fe, Sb, X = Cl, Br, I), significantly improving its photoluminescence capability (figure 6(b)) [91]. Zhang *et al* expanded the types of pseudo-halides (such as N_3^- or CN^-) that can be used for QD ligand exchange, and demonstrated that the azide ligand N_3^- is particularly effective for III–V QDs (such as InAs and InP) [92].

It is noteworthy that halide anions are characterized by exceptionally small dimensions, with ionic sizes of Cl^-, Br^-, and I^- potentially as diminutive as 0.1 nm, substantially smaller than typical organic ligands and metal chalcogenide ligands. For instance, the size of the minimal organic ligand such as ethanedithiol is approximately 0.5 nm, whereas metal chalcogenide ligands, like $Sn_2S_6^{4-}$, measure about 0.7 nm [97]. The shorter ligand can be demonstrated by the shortened spacing between QDs, as shown in figure 6(c). This smaller size allows the ligands to cover the surface of QDs more densely and uniformly, which helps reduce the formation of surface traps and the likelihood of non-radiative auger recombination caused by uneven surface coverage. Both of these issues contribute to photoluminescence intermittency, commonly known as 'blinking' phenomena [98, 99]. Additionally, the smaller ligands enhance the confinement of electrons and holes within the QDs, leading to a stronger quantum confinement effect. This enhanced confinement results in higher luminous efficiency and a narrower emission spectrum in QDs. Particularly for blue light QDs, which require strict quantum confinement effects on size due to their short emission wavelengths [100, 101], halide ligands with their extremely small dimensions are especially ideal for synthesis.

In summary, halides and metal halides provide stronger passivation than ligands such as chalcogenides and are currently the most promising inorganic ligands. In addition, since perovskite materials are usually composed of halogens (I, Br, Cl), as shown in figure 6(d), halide and metal halide ligands are chemically compatible with the perovskite lattice and can be used without destroying the original crystal structure. Integrating into the perovskite lattice or forming stable chemical bonds on its surface, its development has become one of the important driving forces for the application and performance improvement of perovskite QD materials.

3.5. Metal cation

Metal cations that can be used as QD ligands usually include In^{3+}, Cd^{2+}, Zn^{2+}, Pb^{2+}, Li^+, etc [61, 104–106]. According to the Lewis acid–base theory, metal cations, functioning as a Z-type ligand (Lewis acid), can combine with the Lewis basic sites on the surface of QDs. These sites are typically non-metallic sites, forming a completely different binding method from mainstream anionic ligands such as MCC (figure 7(a)). Initially, Page *et al* achieved CdTe QDs with nearly uniform and high PLQY through $CdCl_2$ ligand passivation,

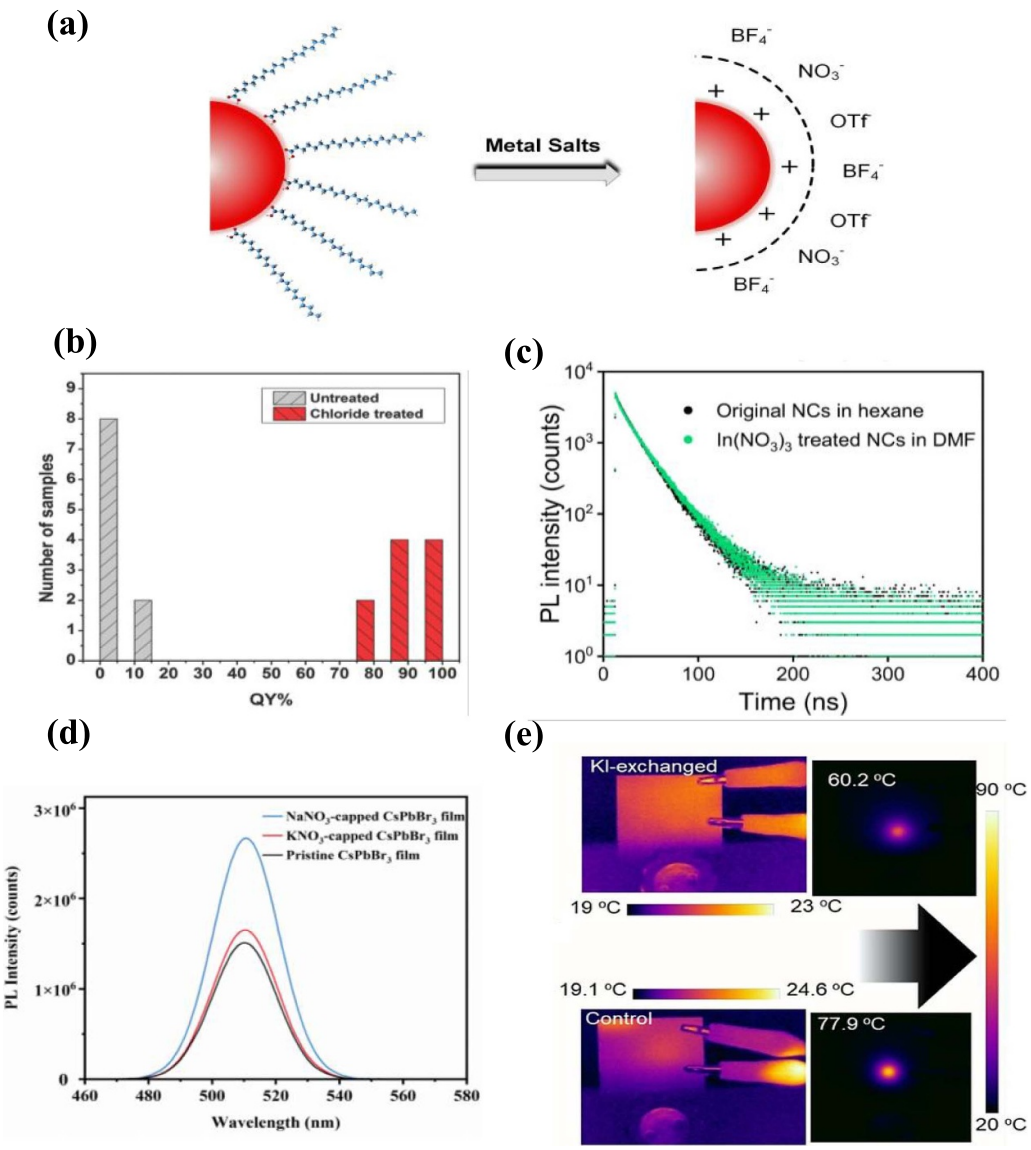

Figure 7. (a) Schematic diagram of metal cation-coordinated QDs and non-coordinated anions as counter ions. Reproduced from [61]. CC BY 4.0. (b) PLQY comparison of CdTe QDs before and after CdCl2 treatment. Reproduced from [107]. CC BY 4.0. (c) Time-resolved PL decay curves of CdSe/CdZnSeS/ZnS NCs before and after treatment with ln^{3+}. Reproduced from [61]. CC BY 4.0. (d) Variations in PL intensity of $CsPbBr_3$ NC films with initial measurements and after K^+ and Na^+ treatments. Reprinted from [109], Copyright (2021), with permission from Elsevier. (e) Maximum operating temperature of K^+ treated QD films. [110]. John Wiley & Sons. (© 2021 Wiley-VCH GmbH).

claiming that it was due to the passivation of Cd sites by Cl^- (figure 7(b)) [107]. Houtepen *et al* speculated based on DFT calculations that the lone pair of electrons on the anionic sites on the QD surface is the main reason for the emergence of trap states. However, L-type and X-type ligands do not have the ability to directly affect the trap state density on the QD surface. Only Z Type ligands can passivate these trap states and change PLQY [108]. So based on this theory, Kirkwood *et al* put forward a new guess about $CdCl_2$ ligand passivation of CdTe QD and proved that Cd^{2+} in $CdCl_2$ achieves passivation of Te site [104].

The latest research by Xiao *et al* proposed the use of metal salts composed of cations such as In^{3+}, Zn^{2+} and Cd^{2+} and non-coordinating anions (such as NO_3^-、BF_4^- or OTf^-) to passivate II–VI semiconductor QDs like CdSe/ZnS, CdSe/CdZnSeS/ZnS and other [61]. This strategy can maintain the QDs luminescence properties and extremely high quantum yield while gently removing the surface original organic ligands (figure 7(c)). In addition, metal cations also show excellent performance in passivating perovskite QDs. Na^+, K^+, Y^+, Gu^+, Pb^{2+}, In^{3+} ions are used to passivate and repair the local trap state of $CsPbI_3$ perovskite QDs [105, 106, 109–112]. Films treated with these metal cations generally demonstrate enhanced luminescence and improved charge transport properties (figure 7(d)) [111]. Besides, these films also display improved stability, enhance heat dissipation, and reduce the maximum operating temperature (figure 7(e)) [110]. However, the use of certain metal cation ligands,

Table 1. Summary of properties of different inorganic ligands.

Ligand type	Advantages	Disadvantages	Applicable fields	Potential for improvement/ research directions
MCC	-Strong electron mobility -High quantum yield	-Requires toxic solvents -Limited solvent options	-Semiconductor devices -Photovoltaics and sensors	-Develop non-toxic synthesis methods -Expand solvent compatibility
MFC	-Environmentally friendly -Simple structure	-High defect state density -Weak hole transport	-Solar cells -Optical glasses and sensors	-Reduce defect state density -Enhance optoelectronic properties
Oxoanions	-Excellent electron storage -Stable bonding	-Weak coordination -Unstable	-Electro catalysts -Solar cell	-Improve core affinity -Expand QD compatibility
Halides	-Fewer defects -Strong electronic coupling -High luminescence efficiency	Not clear	-Perovskite solar cells -Photocatalysis and sensors	-Compatibility with different QDs
Metal Cation	-Enhanced luminescence -Trap passivation	-Toxic and expensive	-QLEDs patterning techniques	-Develop safer metal cations -Reduce synthesis costs

notably Cd^{2+} and Pb^{2+}, which are costly and potentially toxic, raises environmental and health concerns. Consequently, a careful assessment of the benefits and risks is essential prior to their application.

In table 1, we summarize and compare the key properties and applications of the different inorganic ligands discussed above. This overview highlights the distinct advantages and disadvantages associated with each ligand type, providing a clear perspective on their potential use in various QD applications.

4. LED devices based on ILQDs

QD-based QLEDs have shown significant advantages over traditional LEDs and organic LEDs (OLEDs) in the display field (figure 8(a)). These advantages include wider color gamut (figure 8(b)), excellent stability and low production costs, while maintaining similar efficiency levels to OLED [9, 113–115]. By adjusting the size or composition of QDs, the luminescence properties can be precisely controlled without changing the processing process, thus providing great flexibility and potential for the development of multifunctional and high-performance display devices [8, 116–119]. Inorganic ligands, such as the previously discussed halide anions, offer a seamless link between QD properties and their practical applications in display technologies. These ligands facilitate the fine-tuning of QD dimensions and enhance their stability, which are critical for the emission consistency and longevity of display devices. For instance, the small ionic radius of halides allows closer packing and tighter quantum confinement, leading to brighter and more color-precise emissions. This enhanced emission control is essential for the next generation of displays, which require precise color reproduction for improved visual experiences.

The electroluminescence principle of QLEDs relies on its unique device structure and dynamic management of charge carriers. In QLEDs, the typical structure is a p-i-n architecture, in which a thin, single-layer QD film is sandwiched between an n-type electron transport layer (ETL) and a p-type hole transport layer (HTL) (figure 8(c)). This structural design optimizes carrier injection and recombination, resulting in efficient light emission [9, 124–128]. Under forward bias application, electrons from the ETL and holes from the HTL are efficiently injected into the middle QD layer. These carriers meet in the QD layer and form electron–hole pairs. The radiative recombination of these pairs generates photons, which realizes the luminescence of the LED device. By introducing inorganic ligands to replace organic ligands on the QD surface, the deterioration of carrier transport caused by QD stacking of long-chain organic ligands can be improved and the carrier mobility of the QD layer can be greatly improved. Moreover, they can also help maintain the structural integrity and electronic properties of QDs under the electrical stress of operating conditions, which is critical for achieving stable and uniform light emission over prolonged periods. This stability is vital for QLEDs, especially when targeting applications that require consistent color and brightness, such as high-definition displays and advanced lighting systems.

External quantum efficiency (EQE) refers to the ratio of the number of photons emitted from the device to the number of injected electrons and is one of the key indicators for evaluating the performance of QLEDs [13, 129–131]. In Auger recombination, the recombination energy of electron–hole pairs is not released by emitting photons, but is transferred to other electrons or holes and is dissipated in the form of thermal energy or phonon vibration. This energy transfer will lead to a decrease in luminous efficiency. Some researchers have used multi-shell structures to suppress Auger recombination to stabilize EQE and improve brightness [123]. Notably, optimal thicknesses of the inner and outer shells in these core/shell/shell QDs can significantly extend the photoluminescence lifetime, and maximize PLQY [132]. However, the introduction of multi-shell structures increases the complexity of the synthesis process. At the same time, the multi-shell layers may reduce the size effect of QDs, leading to a shift in the

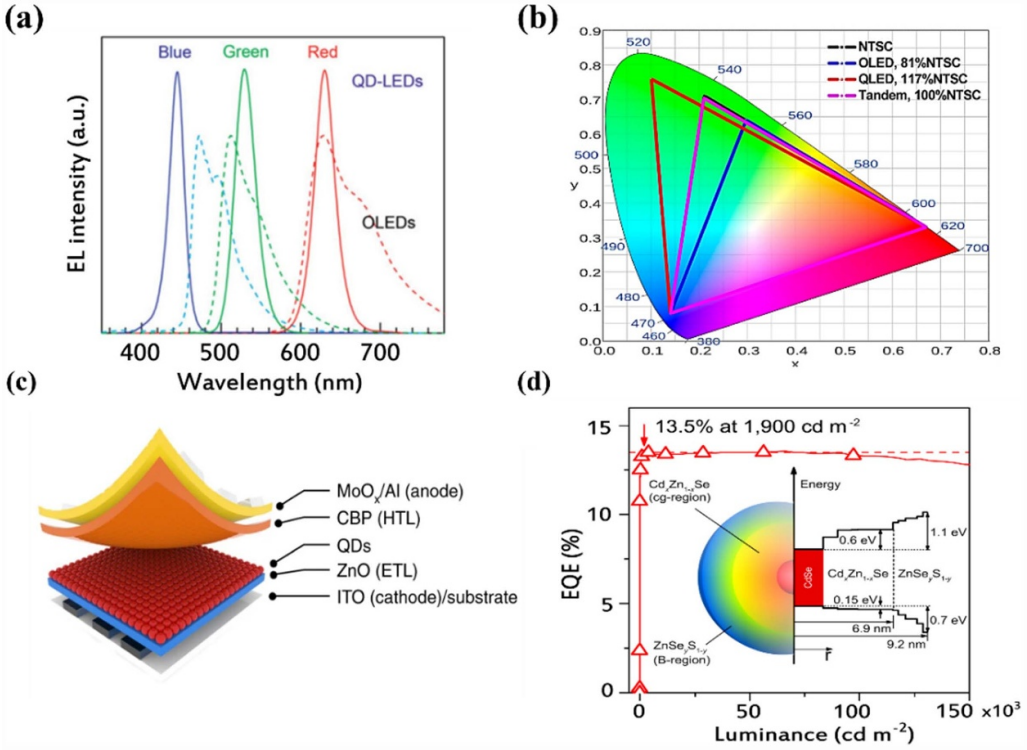

Figure 8. (a) Comparison of the electroluminescence spectra of blue, green, and red QLEDs (solid lines) and OLEDs (dashed lines) at similar wavelengths. Reproduced from [120], with permission from Springer Nature. (b) CIE (International Commission on Illumination) 1931 chromaticity diagram. The triangles respectively represent the NTSC (National Television System Committee) standard (black), OLED (blue), QLED (red), OLED-QLED hybrid series LED (pink) display color gamut. Reprinted with permission from [121]. Copyright (2016) American Chemical Society. (c) Schematic diagram of the electroluminescent QLED structure. Reproduced from [122]. CC BY 4.0. (d) Achieve stable EQE by using multi-shell structures to suppress non-radiative Auger recombination within QDs. Reprinted with permission from [123]. Copyright (2018) American Chemical Society.

emission peak and changes in the emission color. Interfacial trap states at the shell layers can introduce nonradiative pathways, particularly when shell thicknesses are increased beyond an optimal range, subsequently decreasing PLQY [132–134]. In this context, inorganic ligand passivation is particularly important. Inorganic ligand passivation reduces surface defects and impurities that are often the primary cause of nonradiative recombination.

All in all, for the application of QDs in LEDs, effective ligand passivation not only improves the optoelectronic properties of QDs and increases the localization of excitons, but also enhances the chemical and optical stability of QDs, thereby improving overall device performance and lifetime. A large number of studies have shown that ILQDs have high PLQY and excellent charge transport capabilities [61, 80, 92, 135, 136]. Table 2 summarizes the latest research results on inorganic ligand-modified QLEDs, showing their PL and EL properties.

Current research materials of LED prepared by ILQDs is mainly based on perovskite QDs. Halides and pseudohalide inorganic ligands are currently a hot topic in research. By using inorganic halides such as Cl^-, Br^-, I^-, etc, researchers can significantly improve the brightness and luminous efficiency of QLEDs. For example, Li *et al* used chloride ions to passivate the surface of CdSe/ZnS core–shell QDs, which increased the carrier mobility by an order of magnitude and achieved an ultra-high brightness of 460 000 cd·m^{-2} [37]. The latest research has achieved high EQE while meeting the pure red emission wavelength of ultra-high definition displays required by the Rec.2020 standard [159, 160]. Feng *et al* provided a high-performance perovskite LED (PeLED) with an EQE of up to 26.1% by using $PbCl_X^-$ modified $CsPbI_3$ QDs that showed pure red emission (emission center at 638 nm) (figure 9(a)) [145]. The nucleophilic reaction of chloride ions effectively controls the recombination of excitons and suppresses their dissociation due to surface defects. This strategy not only improves the electro-optical performance of the device, but also shows excellent spectral stability under high driving voltage. In addition, some inorganic ligands have been shown to improve LED thermal stability. For example, Wu *et al* compared $CsPbBr_3$ PeLEDs passivated using Br^- and PEABr (figure 9(b)). The Br^- passivated QLED maintained ultra-high stability after multiple high-temperature operating tests (figure 9(c)). The quasi-2D LED made of organic molecule PEABr showed significant degradation (figure 9(d)). The results obtained through the lifetime prediction function show that the T_{50} (the value at which brightness decays to half of its initial value) of the LED exceeds 108 h even at a high brightness of 104 cd·m^{-2} [142]. Additionally, Zheng *et al* reported that by modifying the surface Zn site trap states

Table 2. PL and EL properties of inorganic ligand modified QDs.

Ligands	QDs	EL color	EQE (%)	PLQY (%)	EL Peak (nm)	FWHM (nm)	Von (V)	L_{max} (cd·m^{-2})	τ_{ave}	References
SCN^-	$CsPbBr_3$	Green	17.3	82	521	17	3	48 000	8.06	[137]
SCN^-	$CsPbI_3$	Red	10.3	89	695	52	2.2	823	70.02	[138]
BF_4^-	$CsPbBr_xCl_{3-x}$	Blue	3.2	87	468		3.2	275	11.47	[139]
I^-	$CsPb(I_xBr_{1-x})_3$	Red	24.4	95		30	2.6	760.5		[140]
I^-	$CsPbI_3$	Red	23	96	640	31	2		20	[110]
Br^-	$CsPb(Br_x/Cl_{1-x})_3$	Blue	14.6	95	488	19	3	403	21.08	[141]
Br^-	$CsPbBr_3$	Green	16.2		520		2.4	50 270		[142]
Br^-	InP/ZnS/ZnS	Blue	2.6	93	488	47	2.9	422	95	[143]
Br^-	ZnSeTe/ZnSe/ ZnS	Blue	5.46	86.2	443	22	5.9	332		[144]
Cl^-	$CsPbI_3$	Red	26.1	90	638	36	2.8	2511	10.2	[145]
Cl^-	CdSeZnS–ZnS	Green		75	514	26	2.5	460 000	21	[37]
S2-	Zn–Ag–In–Ga–S	Red	5.32	86.2	628	82		218	531.3	[146]
SO_4^{2-}	$CsPbI_3$	Red	9.94	84	684	62	2.31	2182	112	[147]
SO_4^{2-}	$CsPbI_{3-x}Br_x$	Red	12.6	95	630	27	2.5	5000	37	[148]
K^+	$CsPb(Br_x/Cl_{1-x})_3$	Blue	1.96	38.4	477	19		213		[149]
K^+	(Cs/FA/pF-PEA)$Pb(Cl/Br)_3$	Blue	4.14	34.8	469		3.3	451	12.6	[150]
K^+	(Cs/FA/pF-PEA)$Pb(Cl/Br)_3$	Red	3.55	93	637	31	3.6	2671	30.51	[151]
Na^+	$CsPbBr_3$	Green	17.4	73	512		2.9	8353		[152]
Na^+	$CsPbBr_3$	Blue	12.3	90	479		2.8			[153]
Cs^+–Rb^+	$FAPbI_3$		15.84		405		0.5		1884	[154]
Zn^{2+}	$CsPbBr_3$	Green	6.43	100	512			96 392	15.01	[155]
Cu^{2+}	$CsPbI_3$	Red	2.03	74.2	687		1.6	1270	48	[156]
Mg^{2+}	$CsPbI_3$	Red	8.4	95	686		2.7	672	72.74	[157]
In^{3+}	$CsPbBr_xI_{3-x}$	Red	11.2	99.8	639		2.4	423	2.69	[158]

Abbreviations and their full meanings: PL (photoluminescence), EL (electroluminescent peak), FWHM (full width at half maximum), V_{on} (turn-on voltage), L_{max} (maximum luminance), τ_{ave} (average photoluminescence lifetime).

(figure 9(e)) of ternary ZnSeTe multi-shell QDs with bromide, they achieved a substantial increase in the PLQY from 39.7% to 86.2% and the EQE from 0.74% to 5.46% [144]. In addition, to address the instability problem of mixed halide perovskite ($CsPb(I_xBr_{1-x})_3$) in applications, Wang *et al* proposed an antisolvent-assisted in-situ passivation method using I^-. The metal halide perovskite (MHP) solid has a stability of more than one year under ambient conditions, and the prepared LED has an EQE of 24.4% and a PLQY of 95%, which is currently the longest working stability red PeLED with an EQE of more than 20% (figures 9(f) and (g)) [140]. Although the use of halide passivation can effectively improve the performance of LED devices such as EQE, its long-term stability is still its fatal shortcoming and the biggest challenge in practical applications. Currently, Yang *et al* developed a strategy for QD surface modification using pseudohalogen SCN^-. By using thiocyanate to replace bromide ions, the energy barrier for halide ion migration is increased, bromide ion migration is inhibited, and the LED operating half-life is extended to more than 2 h at a brightness of 1000 cd·m^{-2}, which is 5 times that of traditional LEDs (figure 9(h)). At the same time, the LED exhibits a high maximum EQE of 17.3% (figure 9(i)), a narrow fwhm below 17 nm, and a high maximum brightness of 47 927 cd·m^{-2} [137].

In addition, research on metal cation ligands in QLED has also achieved breakthroughs. Yang *et al* promoted the bonding of bromine sites on the $CsPbI_{3-x}Br_x$ surface with K^+ by creating a potassium-rich environment, reducing the defect density on the halide-rich surface and inhibiting halide migration (figure 10(a)). Achieved a PLQY of 93% and a high EQE of 3.55% [151]. In recent years, a large number of studies have shown that halide defects (halide dangling bonds or halide gaps) present in the contact interface between the grain boundaries of QD films and the charge transport layer can cause severe non-radiative recombination losses and limit the improvement of LED luminescent efficiency [161–163]. Shen *et al* proposed a strategy to use K^+ to induce the growth of QD films on a PEDOT:PSS HTL crystalline substrate, which can suppress the defect state at the interface between the QD layer and the HTL layer to solve the problem of hole transport obstruction and the resulting fluorescence quenching problem (figure 10(b)). They finally achieved a peak EQE of 4.14% and a current efficiency (CE) of 2.71 cd·A^{-1} [150]. Furthermore, the imbalance between electron mobility and hole mobility between the ETL and the HTL is a problem that cannot be ignored in LED applications. Studies have shown that the mismatch in carrier mobility may lead to serious problems such as charge accumulation and device performance degradation [164–169]. In response to this issue, Chen and his colleagues improved the charge transport balance within the device by replacing the original PEA ligands in the $CsPbBr_3$ films with Na^+, which slightly increased the hole mobility and at the

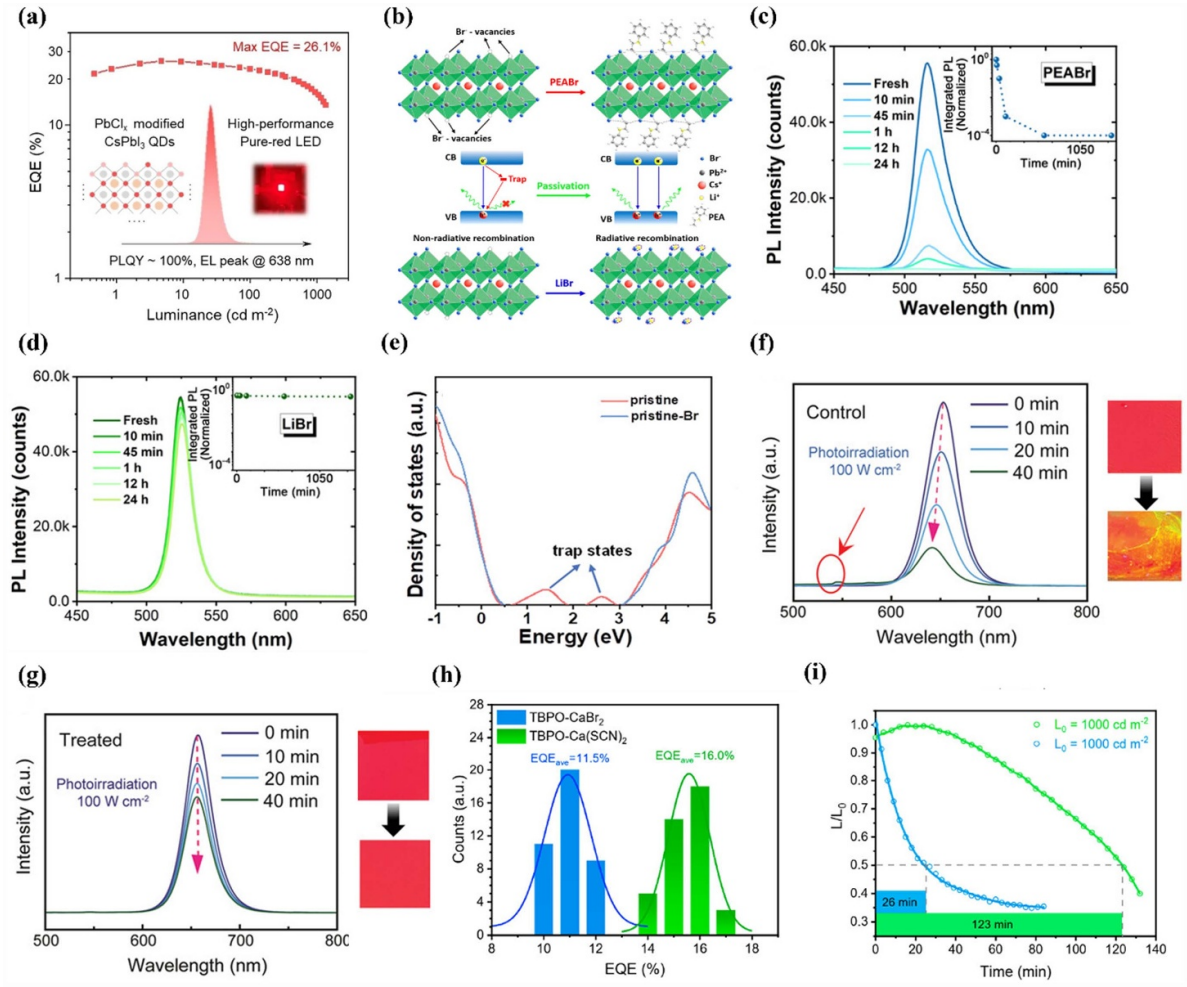

Figure 9. (a) Electroluminescence properties of $PbCl_X^-$ modified $CsPbI_3$ QDs. [145] John Wiley & Sons. (© 2024 Wiley-VCH GmbH). (b) Schematic diagram of the surface vacancies and passivation of PEABr organic ligands and LiBr inorganic ligands on the surface of $CsPbBr_3$ perovskite film. (c), (d) Time-dependent PL spectra and integrated PL intensity of perovskite films treated with PEABr (c) and LiBr (d) and annealed at 120 °C (inset). [142] John Wiley & Sons. (© 2019 Wiley-VCH Verlag GmbH & Co. KGaA, Weinheim). (e) Comparison of the shell state density of original and Br^- modified ZnSeTe/ZnSe/ZnS QDs ZnS. Reproduced from [144]. CC BY 4.0. (f), (g) Stability of untreated (f) and I–ion passivated (g) $CsPb(I_xBr_{1-x})_3$ MHP films under 100 W·cm^{-2} light irradiation, the right side of the picture shows the color change of the film after one week. [140] John Wiley & Sons. (© 2022 Wiley-VCH GmbH). (h) Histogram of the maximum EQE of 40 LED devices fabricated using Br^- and SCN^- coordinated QDs respectively. (i) Comparison of the working life of LED devices fabricated using Br^-(blue) and SCN^-(green) coordinated QDs at a brightness of 1000 cd·cm^{-2}. Reprinted with permission from [137]. Copyright (2023) American Chemical Society.

same time enhanced the electron mobility by an order of magnitude (figure 10(c)) .This makes the charge transfer in the device more balanced [152].

In current research on QLEDs, the organic ligand co-passivation strategy has proven to be an extremely effective strategy. Through the comprehensive use of organic–inorganic hybrid ligands (OIHL), which combines the characteristics and advantages of both, superior overall device performance can be achieved compared to using either organic or inorganic ligands alone for passivation.

For example, Kim *et al* reduced the crystal size and the number of surface defects by introducing multi-organic ligand-KBr double passivation in $CsPbBr_xI_{3-x}$ (figure 10(d)), thereby reducing the diffusion length and non-radiative recombination of excitons. This strategy successfully developed high-performance red PeLEDs with an EQE of 10.2%, abrightness of 743.2 cd·m^{-2} [2], and a CE of 3.2 cd·A, while possessing a low turn-on voltage of 1.6 V and pure red emission characteristics [170]. In another study, enhancement of luminescence characteristics and carrier injection can be achieved by introducing high-valent metal bromide (MBr_n) inorganic ligands to replace part of the OTAc and DDAB ligands on the surface of QDs. This method not only improves the photoelectric performance of QLED, but also achieves a peak EQE of 16.48%. In addition, the universal applicability of the OIHL strategy was further verified, demonstrating that the use of various metal bromides such as $MnBr_2$, $GaBr_3$, and $InBr_3$ can improve device performance by nearly 40% (figure 10(e)) [171].

In addition, the passivation strategy of benzoic acid (BA^-)-alkali metal ions (Li^+, Na^+, K^+) was successfully applied in the blue-light mixed halide perovskite $CsPbI_{3-x}Br_x$ [172].

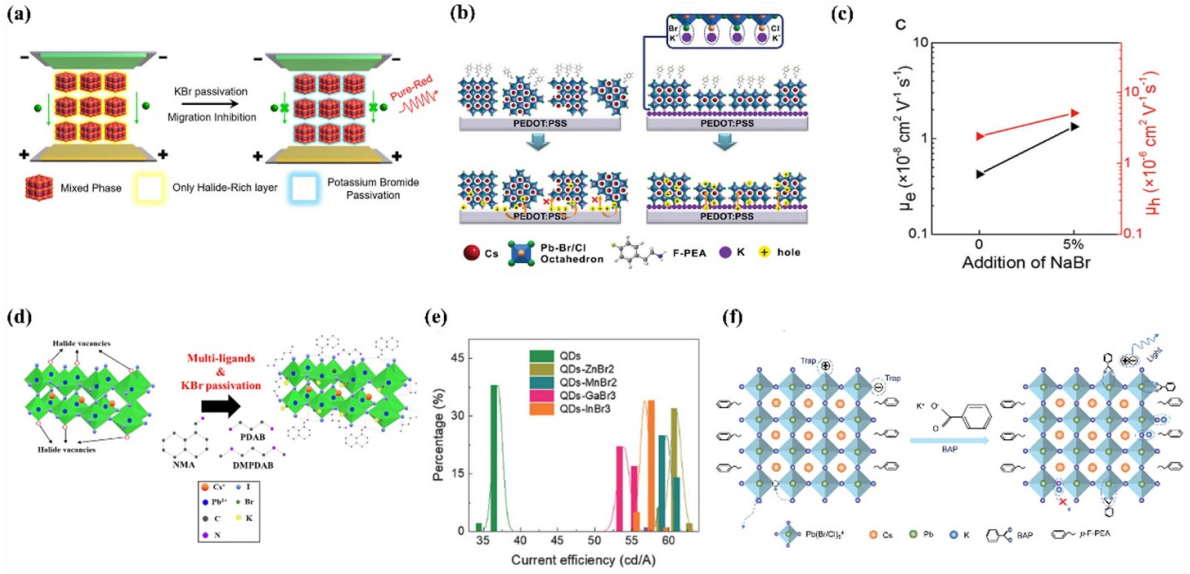

Figure 10. (a) Schematic diagram of potassium ion ligand QDs inhibiting the migration of halogen ions (green balls are halogen ions). Reprinted with permission from [151]. Copyright (2020) American Chemical Society. (b) Comparison of hole transport behavior whether the interface between QDs and HTL is modified with K^+. [150] John Wiley & Sons. (© 2020 Wiley-VCH GmbH). (c) Effect of Na^+ modification on hole and electron mobility. [152] John Wiley & Sons. (© 2019 WILEY-VCH Verlag GmbH & Co. KGaA, Weinheim). (d) Mechanism of multi-organic ligand-KBr double passivated perovskite QDs. Reprinted from [170], Copyright (2021), with permission from Elsevier. (e) Average peak current efficiency histogram of 40 QLED devices with different bromides as ligands. [171] John Wiley & Sons. (© 2018 WILEY-VCH Verlag GmbH & Co. KGaA, Weinheim). (f) Schematic diagram of the coordination of BA^- and K^+ with Pb and halide sites respectively. [172] John Wiley & Sons. (© 2023 Wiley-VCH GmbH).

This strategy utilizes BA^- groups to coordinate with under-coordinated Pb atoms, greatly reducing trap-mediated non-radiative recombination caused by halide vacancies. At the same time, the strong ionic bonds formed between alkali metal ions and halide atoms reduce the migration of halide ions and enhance the overall stability and luminous efficiency of the material (figure 10(f)). A sky-blue PeLED constructed with organic–inorganic bifunctional ligand QD materials exhibits EL peak emission at 483 nm and reaches an EQE of 16.58% and a maximum EQE of 18.65%. After the optical output coupling is enhanced, the EQE is further improved to 28.82%. Further research and development of organic–inorganic ligand co-passivation strategies will play an important role in promoting the industrialization and commercial application of perovskite QLEDs in the future.

5. Summary and Perspectives

As QD technology continues to advance, research and development of QLEDs have significantly enhanced the performance of display technologies and optoelectronic devices. By precisely controlling the size, shape, and composition of QDs, researchers can optimize the emissive properties of devices to meet the stringent requirements of high-resolution displays and efficiency photovoltaic devices. Notably, inorganic ligand passivation strategies play a crucial role in enhancing the stability and electro-optical performance of QDs, enabling QLEDs to achieve commercial standards in brightness, efficiency, and longevity. This article provides a comprehensive review of the mechanisms of inorganic ligand exchange in QDs, utilizing solution-phase ligand exchange techniques to gently remove surface organic ligands and achieve strong binding with inorganic ligands. It further summarizes the types and characteristics of various inorganic ligands, including MCC, MFC, oxoanions, halides, and metal cations. Finally, it outlines the latest research advancements in LEDs using various inorganic-ligand-capped QDs, highlighting their beneficial impacts on QLED performance and potential in future applications.

While inorganic ligands provide an effective means for surface passivation and functionalization of QDs, there are still challenges and limitations. Currently, the number of developed inorganic ligands is not as abundant as organic ligands, and many promising materials remain unexplored. For instance, metal cyanides with good electron-donating properties ($Co(CN)_6^{3-}$, $Fe(CN)_6^{4-}$) [173–175], highly electronegative and stable metal fluoroborates ($AgBF_4$, $NiBF_4$) [176, 177], biocompatible fluorophosphates (PF^{5-}), [178] rare earth elements often used as dopants to adjust the properties of NCs [179] and lanthanide elements commonly used in luminescent and magnetic nanomaterials, [180] etc.

Most of the current research is based on a single inorganic ligand, so the effects and advantages of multiple ligands can be combined by using multiple ligands for passivation simultaneously and synergistically. For example, using NH_4^+ alone to passivate $CsPb(Br/Cl)_3$ can only obtain a maximum PLQY of 12%. However, combining NH_4^+ with $CaCl_2$, where ammonium ions fill surface vacancies of cesium and calcium halide creates a halide-rich environment acting as a ligand with

surface halide atoms, can achieve up to 93% PLQY [181]. In addition, as mentioned before, the organic–inorganic dual ligand strategy is also a new research method for multi-ligand passivation.

In the development of RGB (red, green, blue) QLEDs, the performance of state-of-the-art blue light QLEDs still lags behind red and green QLEDs. Using mixed halide perovskite materials for blue light, due to the high mobility and small ionic radius of Cl^- ions, it is difficult to achieve high QD directional fluorescence emission, resulting in generally low PLQY [182–185]. Inorganic ligands, such as metal sulfides, metal cations, etc, can effectively inhibit the migration of chloride ions due to their strong chemical bonding energy and stable chemical properties. Therefore, further research on inorganic ligand passivation strategies may be the key to achieving breakthroughs in blue-light QLED performance in the future.

Photolithography technology is the preferred method for high-resolution patterning processes in the electronics industry due to its ability to precisely control patterns at the micro and nanoscale [186–191]. The direct optical lithography of functional inorganic nanomaterials method combines the advantages of traditional photolithography with the functionality of inorganic nanomaterials to provide an efficient and cost-effective patterning solution [122, 192–198]. Inorganic ligands can not only ensure the stability of QDs in colloidal solutions, but also react with photochemically active additives when irradiated with light, changing the solubility of QDs in solvents. At the same time, they avoid organic photolithography. The use of glue and other by-product dilution or contamination can significantly improve the charge transport performance and stability, thus showing great application potential in direct optical patterning technology.

In summary, inorganic ligands not only improve the stability and electro-optical properties of QDs, but also promote the commercialization of QLED technology. With the further development of inorganic ligand technology, we foresee that QLED will play a more important role in high-resolution display technology and high-efficiency photoelectric conversion devices.

Data availability statement

All data that support the findings of this study are included within the article (and any supplementary files).

Acknowledgments

This work is supported by the National Natural Science Foundation of China (52106089).

Conflict of interest

The authors declare no competing financial interest.

ORCID iDs

Tianxu Zhang https://orcid.org/0009-0008-4422-3368
Bin Xie https://orcid.org/0000-0001-9031-5900
Xiaobing Luo https://orcid.org/0000-0002-6423-9868

References

[1] Alivisatos A P 1996 Semiconductor clusters, nanocrystals, and quantum dots *Science* **271** 933–7
[2] Bawendi M G, Carroll P J, Wilson W L and Brus L E 1992 Luminescence properties of CdSe quantum crystallites: resonance between interior and surface localized states *J. Chem. Phys.* **96** 946–54
[3] Ekimov A I, Efros A L and Onushchenko A A 1985 Quantum size effect in semiconductor microcrystals *Solid State Commun.* **56** 921–4
[4] Rossetti R, Hull R, Gibson J M and Brus L E 1985 Excited electronic states and optical spectra of ZnS and CdS crystallites in the ≈15–50 Å size range: evolution from molecular to bulk semiconducting properties *J. Chem. Phys.* **82** 552–9
[5] Brus L 1986 Electronic wave functions in semiconductor clusters: experiment and theory *J. Phys. Chem.* **90** 2555–60
[6] Colvin V L, Schlamp M C and Alivisatos A P 1994 Light-emitting diodes made from cadmium selenide nanocrystals and a semiconducting polymer *Nature* **370** 354–7
[7] Kim T, Kim K-H, Kim S, Choi S-M, Jang H, Seo H-K, Lee H, Chung D-Y and Jang E 2020 Efficient and stable blue quantum dot light-emitting diode *Nature* **586** 385
[8] Shirasaki Y, Supran G J, Bawendi M G and Bulović V 2013 Emergence of colloidal quantum-dot light-emitting technologies *Nat. Photon.* **7** 13–23
[9] García de Arquer F P, Talapin D V, Klimov V I, Arakawa Y, Bayer M and Sargent E H 2021 Semiconductor quantum dots: technological progress and future challenges *Science* **373** eaaz8541
[10] Li Y Q, Rizzo A, Mazzeo M, Carbone L, Manna L, Cingolani R and Gigli G 2005 White organic light-emitting devices with CdSe/ZnS quantum dots as a red emitter *J. Appl. Phys.* **97** 113501
[11] Xu J, Cui D H, Lewis B A, Wang A Y, Xu S Y and Gerhold M 2005 Microcavity light-emitting devices based on colloidal semiconductor nanocrystal quantum dots *IEEE Photonics Technol. Lett.* **17** 2008–10
[12] Kim T-H *et al* 2011 Full-colour quantum dot displays fabricated by transfer printing *Nat. Photon.* **5** 176–82
[13] Liu Z *et al* 2020 Micro-light-emitting diodes with quantum dots in display technology *Light Sci. Appl.* **9** 83
[14] Sun Q, Wang Y A, Li L S, Wang D, Zhu T, Xu J, Yang C and Li Y 2007 Bright, multicoloured light-emitting diodes based on quantum dots *Nat. Photon.* **1** 717–22
[15] Jang H J, Lee J Y, Baek G W, Kwak J and Park J-H 2022 Progress in the development of the display performance of AR, VR, QLED and OLED devices in recent years *J. Inf. Dis.* **23** 1–17
[16] Hu L, Zhao Q, Huang S, Zheng J, Guan X, Patterson R, Kim J, Shi L, Lin C-H and Lei Q 2021 Flexible and efficient perovskite quantum dot solar cells via hybrid interfacial architecture *Nat. Commun.* **12** 466
[17] Memari A, Javadian Sarraf M, Chabok S J S M and Motevalizadeh L 2023 Comprehensive guidance for optimizing the colloidal quantum dot (CQD) Perovskite solar cells: experiment and simulation *Sci. Rep.* **13** 16675
[18] Yang Z *et al* 2017 Mixed-quantum-dot solar cells *Nat. Commun.* **8** 1325
[19] Chuang C-H M, Brown P R, Bulović V and Bawendi M G 2014 Improved performance and stability in quantum dot

solar cells through band alignment engineering *Nat. Mater.* **13** 796–801
[20] Bakalova R, Zhelev Z, Aoki I and Kanno I 2007 Designing quantum-dot probes *Nat. Photon.* **1** 487–9
[21] Liu J *et al* 2022 A near-infrared colloidal quantum dot imager with monolithically integrated readout circuitry *Nat. Electron.* **5** 443–51
[22] Roy P, Virmani M and Pillai P P 2023 Blue-emitting InP quantum dots participate in an efficient resonance energy transfer process in water *Chem. Sci.* **14** 5167–76
[23] Zhou W *et al* 2020 Solution-processed upconversion photodetectors based on quantum dots *Nat. Electron.* **3** 251
[24] Chen Y, Yu S, Fan X-B, Wu L-Z and Zhou Y 2023 Mechanistic insights into the influence of surface ligands on quantum dots for photocatalysis *J. Mater. Chem.* A **11** 8497–514
[25] Xu L, Li J, Cai B, Song J, Zhang F, Fang T and Zeng H 2020 A bilateral interfacial passivation strategy promoting efficiency and stability of perovskite quantum dot light-emitting diodes *Nat. Commun.* **11** 3902
[26] Shrestha A, Batmunkh M, Tricoli A, Qiao S Z and Dai S 2019 Near-infrared active lead chalcogenide quantum dots: preparation, post-synthesis ligand exchange, and applications in solar cells *Angew. Chem., Int. Ed.* **58** 5202–24
[27] Heuer-Jungemann A *et al* 2019 The role of ligands in the chemical synthesis and applications of inorganic nanoparticles *Chem. Rev.* **119** 4819–80
[28] Kagan C R and Murray C B 2015 Charge transport in strongly coupled quantum dot solids *Nat. Nanotechnol.* **10** 1013–26
[29] Lee S, Choi M-J, Sharma G, Biondi M, Chen B, Baek S-W, Najarian A M, Vafaie M, Wicks J and Sagar L K 2020 Orthogonal colloidal quantum dot inks enable efficient multilayer optoelectronic devices *Nat. Commun.* **11** 4814
[30] Zito J and Infante I 2021 The future of ligand engineering in colloidal semiconductor nanocrystals *Acc. Chem. Res.* **54** 1555–64
[31] Peña L F, Koepke J C, Dycus J H, Mounce A, Baczewski A D, Jacobson N T and Bussmann E 2024 Modeling Si/SiGe quantum dot variability induced by interface disorder reconstructed from multiperspective microscopy *npj Quantum Inf.* **10** 33
[32] Kavrik M S, Hachtel J A, Ko W, Qian C, Abelson A, Unlu E B, Kashyap H, Li A-P, Idrobo J C and Law M 2022 Emergence of distinct electronic states in epitaxially-fused PbSe quantum dot superlattices *Nat. Commun.* **13** 6802
[33] Kroupa D M, Voros M, Brawand N P, McNichols B W, Miller E M, Gu J, Nozik A J, Sellinger A, Galli G and Beard M C 2017 Tuning colloidal quantum dot band edge positions through solution-phase surface chemistry modification *Nat. Commun.* **8** 15257
[34] Wang L, Lv Y, Lin J, Zhao J, Liu X, Zeng R, Wang X and Zou B 2021 Surface organic ligand-passivated quantum dots: toward high-performance light-emitting diodes with long lifetimes *J. Mater. Chem.* C **9** 2483–90
[35] Anderson N C, Hendricks M P, Choi J J and Owen J S 2013 Ligand exchange and the stoichiometry of metal chalcogenide nanocrystals: spectroscopic observation of facile metal-carboxylate displacement and binding *J. Am. Chem. Soc.* **135** 18536–48
[36] Liu M, Tang G, Liu Y and Jiang F-L 2024 Ligand exchange of quantum dots: a thermodynamic perspective *J. Phys. Chem. Lett.* **15** 1975–84
[37] Li X *et al* 2018 Bright colloidal quantum dot light-emitting diodes enabled by efficient chlorination *Nat. Photon.* **12** 159
[38] Aqoma H, Lee S-H, Imran I F, Hwang J-H, Lee S-H and Jang S-Y 2024 Alkyl ammonium iodide-based ligand exchange strategy for high-efficiency organic-cation perovskite quantum dot solar cells *Nat. Energy* **9** 324–32
[39] Liu M, Yazdani N, Yarema M, Jansen M, Wood V and Sargent E H 2021 Colloidal quantum dot electronics *Nat. Electron.* **4** 548–58
[40] Kovalenko M V, Scheele M and Talapin D V 2009 Colloidal nanocrystals with molecular metal chalcogenide surface ligands *Science* **324** 1417–20
[41] Kwon S G and Hyeon T 2011 Formation mechanisms of uniform nanocrystals via hot-injection and heat-up methods *Small* **7** 2685–702
[42] Wu W and Shevchenko E V 2018 The surface science of nanoparticles for catalysis: electronic and steric effects of organic ligands *J. Nanopart. Res.* **20** 255
[43] Zherebetskyy D, Scheele M, Zhang Y, Bronstein N, Thompson C, Britt D, Salmeron M, Alivisatos P and Wang L-W 2014 Hydroxylation of the surface of PbS nanocrystals passivated with oleic acid *Science* **344** 1380–4
[44] Yin Y and Alivisatos A P 2005 Colloidal nanocrystal synthesis and the organic–inorganic interface *Nature* **437** 664–70
[45] Murray C, Norris D J and Bawendi M G 1993 Synthesis and characterization of nearly monodisperse CdE (E= sulfur, selenium, tellurium) semiconductor nanocrystallites *J. Am. Chem. Soc.* **115** 8706–15
[46] Deutsch D S, Siani A, Fanson P T, Hirata H, Matsumoto S, Williams C T and Amiridis M D 2007 FT-IR investigation of the thermal decomposition of Poly(amidoamine) dendrimers and dendrimer−metal nanocomposites supported on Al_2O_3 and ZrO_2 *J. Phys. Chem.* C **111** 4246–55
[47] Niu Z, Becknell N, Yu Y, Kim D, Chen C, Kornienko N, Somorjai G A and Yang P 2016 Anisotropic phase segregation and migration of Pt in nanocrystals en route to nanoframe catalysts *Nat. Mater.* **15** 1188–94
[48] Li D, Wang C, Tripkovic D, Sun S, Markovic N M and Stamenkovic V R 2012 Surfactant removal for colloidal nanoparticles from solution synthesis: the effect on catalytic performance *ACS Catal.* **2** 1358–62
[49] Zhang L *et al* 2015 Platinum-based nanocages with subnanometer-thick walls and well-defined, controllable facets *Science* **349** 412–6
[50] Doris S E, Lynch J J, Li C, Wills A W, Urban J J and Helms B A 2014 Mechanistic insight into the formation of cationic naked nanocrystals generated under equilibrium control *J. Am. Chem. Soc.* **136** 15702–10
[51] Nelson A, Zong Y, Fritz K E, Suntivich J and Robinson R D 2019 Assessment of soft ligand removal strategies: alkylation as a promising alternative to high-temperature treatments for colloidal nanoparticle surfaces *ACS Mater. Lett.* **1** 177–84
[52] Elliott E W III, Glover R D and Hutchison J E 2015 Removal of thiol ligands from surface-confined nanoparticles without particle growth or desorption *ACS Nano* **9** 3050–9
[53] Aliaga C, Park J Y, Yamada Y, Lee H S, Tsung C-K, Yang P and Somorjai G A 2009 Sum frequency generation and catalytic reaction studies of the removal of organic capping agents from Pt nanoparticles by UV−ozone treatment *J. Phys. Chem.* C **113** 6150–5
[54] Crespo-Quesada M, Andanson J-M, Yarulin A, Lim B, Xia Y and Kiwi-Minsker L 2011 UV–ozone cleaning of supported poly(vinylpyrrolidone)-stabilized palladium nanocubes: effect of stabilizer removal on morphology and catalytic behavior *Langmuir* **27** 7909–16
[55] Shaw S, Colaux J L, Hay J L, Peiris F C and Cademartiri L 2016 Building materials from colloidal nanocrystal arrays: evolution of structure, composition, and mechanical

properties upon the removal of ligands by O_2 plasma *Adv. Mater.* **28** 8900–5
[56] Wang L, Zhang B and Rui Q 2018 Plasma-induced vacancy defects in oxygen evolution cocatalysts on Ta_3N_5 photoanodes promoting solar water splitting *ACS Catal.* **8** 10564–72
[57] Mohapatra P, Shaw S, Mendivelso-Perez D, Bobbitt J M, Silva T F, Naab F, Yuan B, Tian X, Smith E A and Cademartiri L 2017 Calcination does not remove all carbon from colloidal nanocrystal assemblies *Nat. Commun.* **8** 2038
[58] Niu Z and Li Y 2014 Removal and utilization of capping agents in nanocatalysis *Chem. Mater.* **26** 72–83
[59] Rossi L M, Fiorio J L, Garcia M A S and Ferraz C P 2018 The role and fate of capping ligands in colloidally prepared metal nanoparticle catalysts *Dalton Trans.* **47** 5889–915
[60] Wang W, Zhang M, Pan Z, Biesold G M, Liang S, Rao H, Lin Z and Zhong X 2022 Colloidal inorganic ligand-capped nanocrystals: fundamentals, status, and insights into advanced functional nanodevices *Chem. Rev.* **122** 4091–162
[61] Xiao P, Zhang Z, Ge J, Deng Y, Chen X, Zhang J-R, Deng Z, Kambe Y, Talapin D V and Wang Y 2023 Surface passivation of intensely luminescent all-inorganic nanocrystals and their direct optical patterning *Nat. Commun.* **14** 49
[62] Green M L H 1995 A new approach to the formal classification of covalent compounds of the elements *J. Organomet Chem.* **500** 127–48
[63] Green M L H and Parkin G 2014 Application of the covalent bond classification method for the teaching of inorganic chemistry *J. Chem. Educ.* **91** 807–16
[64] Owen J 2015 The coordination chemistry of nanocrystal surfaces *Science* **347** 615–6
[65] De Roo J, De Keukeleere K, Hens Z and Van Driessche I 2016 From ligands to binding motifs and beyond; the enhanced versatility of nanocrystal surfaces *Dalton Trans.* **45** 13277–83
[66] De Roo J 2023 The surface chemistry of colloidal nanocrystals capped by organic ligands *Chem. Mater.* **35** 3781–92
[67] Jiang C, Lee J-S and Talapin D V 2012 Soluble precursors for $CuInSe_2$, $CuIn_{1-x}Ga_xSe_2$, and $Cu_2ZnSn(S,Se)_4$ based on colloidal nanocrystals and molecular metal chalcogenide surface ligands *J. Am. Chem. Soc.* **134** 5010–3
[68] Mitzi D B, Kosbar L L, Murray C E, Copel M and Afzali A 2004 High-mobility ultrathin semiconducting films prepared by spin coating *Nature* **428** 299–303
[69] Scalise E, Srivastava V, Janke E, Talapin D, Galli G and Wippermann S 2018 Surface chemistry and buried interfaces in all-inorganic nanocrystalline solids *Nat. Nanotechnol.* **13** 841–48
[70] Jung S M, Kang H L, Won J K, Kim J, Hwang C, Ahn K, Chung I, Ju B-K, Kim M-G and Park S K 2018 High-performance quantum dot thin-film transistors with environmentally benign surface functionalization and robust defect passivation *ACS Appl. Mater. Interfaces* **10** 3739–49
[71] Bodnarchuk M I, Yakunin S, Piveteau L and Kovalenko M V 2015 Host–guest chemistry for tuning colloidal solubility, self-organization and photoconductivity of inorganic-capped nanocrystals *Nat. Commun.* **6** 10142
[72] Xia Z *et al* 2015 Generalized water-processed metal chalcogenide complexes: synthesis and applications *Chem. Mater.* **27** 8048–57
[73] Nag A, Chung D S, Dolzhnikov D S, Dimitrijevic N M, Chattopadhyay S, Shibata T and Talapin D V 2012 Effect of metal ions on photoluminescence, charge transport, magnetic and catalytic properties of all-inorganic colloidal nanocrystals and nanocrystal solids *J. Am. Chem. Soc.* **134** 13604–15
[74] Portner J C 2023 *Electrostatic Stabilization and Self Assembly of Charged Colloidal Nanocrystals* (The University of Chicago)
[75] Kovalenko M V, Bodnarchuk M I, Zaumseil J, Lee J-S and Talapin D V 2010 Expanding the chemical versatility of colloidal nanocrystals capped with molecular metal chalcogenide ligands *J. Am. Chem. Soc.* **132** 10085–92
[76] Yuan M, Liu M and Sargent E H 2016 Colloidal quantum dot solids for solution-processed solar cells *Nat. Energy* **1** 1–9
[77] Coropceanu I *et al* 2022 Self-assembly of nanocrystals into strongly electronically coupled all-inorganic supercrystals *Science* **375** 1422–6
[78] Jeong H *et al* 2017 Transition metal-based thiometallates as surface ligands for functionalization of all-inorganic nanocrystals *Chem. Mater.* **29** 10510–7
[79] Ban H W, Park S, Jeong H, Gu D H, Jo S, Park S H, Park J and Son J S 2016 Molybdenum and tungsten sulfide ligands for versatile functionalization of all-inorganic nanocrystals *J. Phys. Chem. Lett.* **7** 3627–35
[80] Nag A, Kovalenko M V, Lee J-S, Liu W, Spokoyny B and Talapin D V 2011 Metal-free inorganic ligands for colloidal nanocrystals: S^{2-}, HS^-, Se^{2-}, HSe^-, Te^{2-}, HTe^-, TeS_3^{2-}, OH^-, and NH^{2-} as surface ligands *J. Am. Chem. Soc.* **133** 10612–20
[81] Oh S J, Berry N E, Choi J-H, Gaulding E A, Lin H, Paik T, Diroll B T, Muramoto S, Murray C B and Kagan C R 2014 Designing high-performance PbS and PbSe nanocrystal electronic devices through stepwise, post-synthesis, colloidal atomic layer deposition *Nano Lett.* **14** 1559–66
[82] Gurin V S and Artemyev M V 1994 CdS quantum dots in colloids and polymer matrices: electronic structure and photochemical properties *J. Cryst. Growth* **138** 993–7
[83] Huang J, Liu W, Dolzhnikov D S, Protesescu L, Kovalenko M V, Koo B, Chattopadhyay S, Shenchenko E V and Talapin D V 2014 Surface functionalization of semiconductor and oxide nanocrystals with small inorganic oxoanions (PO_4^{3-}, MoO_4^{2-}) and polyoxometalate ligands *ACS Nano* **8** 9388–402
[84] Wang W, Pan Z, Rao H, Zhang G, Song H, Zhang Z and Zhong X 2020 Proton initiated ligand exchange reactions for colloidal nanocrystals functionalized by inorganic ligands with extremely weak coordination ability *Chem. Mater.* **32** 630–7
[85] Dos Santos A P and Levin Y 2010 Surface tensions and surface potentials of acid solutions *J. Chem. Phys.* **133** 15
[86] Kleinpeter E and Holzberger A 2006 Structure, intramolecular flexibility, and complexation of aza crown ethers to anions $H_2PO_4^-$ and HSO_4^- in nonprotic solvents *Tetrahedron* **62** 10237–47
[87] Subramanian V and Ducker W A 2000 Counterion effects on adsorbed micellar shape: experimental study of the role of polarizability and charge *Langmuir* **16** 4447–54
[88] Ziyaadini M, Zahedi M M and Dehghan-Rahimi A 2018 Enhanced photocatalytic degradation of 2, 4-dichlorophenol in water solution using Sr-doped $ZnAl_2O_4$ nanoparticles *J. Part. Sci. Technol.* **4** 101–9
[89] Fafarman A T, Koh W-K, Diroll B T, Kim D K, Ko D-K, Oh S J, Ye X, Doan-Nguyen V, Crump M R and Reifsnyder D C 2011 Thiocyanate-capped nanocrystal colloids: vibrational reporter of surface chemistry and solution-based route to enhanced coupling in nanocrystal solids *J. Am. Chem. Soc.* **133** 15753–61
[90] Niu G, Wang L, Gao R, Li W, Guo X, Dong H and Qiu Y 2013 Inorganic halogen ligands in quantum dots: I^-, Br^-, Cl^- and film fabrication through electrophoretic deposition *Phys. Chem. Chem. Phys.* **15** 19595–600

[91] Dirin D N, Dreyfuss S, Bodnarchuk M I, Nedelcu G, Papagiorgis P, Itskos G and Kovalenko M V 2014 Lead halide perovskites and other metal halide complexes as inorganic capping ligands for colloidal nanocrystals *J. Am. Chem. Soc.* **136** 6550–3

[92] Zhang H, Jang J, Liu W and Talapin D V 2014 Colloidal nanocrystals with inorganic halide, pseudohalide, and halometallate ligands *ACS Nano* **8** 7359–69

[93] Ning Z, Dong H, Zhang Q, Voznyy O and Sargent E H 2014 Solar cells based on inks of n-type colloidal quantum dots *ACS Nano* **8** 10321–7

[94] Kim D K, Lai Y, Diroll B T, Murray C B and Kagan C R 2012 Flexible and low-voltage integrated circuits constructed from high-performance nanocrystal transistors *Nat. Commun.* **3** 1216

[95] Choi J-H, Fafarman A T, Oh S J, Ko D-K, Kim D K, Diroll B T, Muramoto S, Gillen J G, Murray C B and Kagan C R 2012 Bandlike transport in strongly coupled and doped quantum dot solids: a route to high-performance thin-film electronics *Nano Lett.* **12** 2631–8

[96] Koh W-K, Saudari S R, Fafarman A T, Kagan C R and Murray C B 2011 Thiocyanate-capped PbS nanocubes: ambipolar transport enables quantum dot based circuits on a flexible substrate *Nano Lett.* **11** 4764–7

[97] Tang J *et al* 2011 Colloidal-quantum-dot photovoltaics using atomic-ligand passivation *Nat. Mater.* **10** 765–71

[98] Efros A L and Nesbitt D J 2016 Origin and control of blinking in quantum dots *Nat. Nanotechnol.* **11** 661–71

[99] Kuang Y, Zhu C, He W, Wang X, He Y, Ran X and Guo L 2020 Regulated exciton dynamics and optical properties of single perovskite $CsPbBr_3$ quantum dots by diluting surface ligands *J. Phys. Chem.* C **124** 23905–12

[100] Wen G, Lin J, Jiang H and Chen Z 1995 Quantum-confined Stark effects in semiconductor quantum dots *Phys. Rev.* B **52** 5913

[101] Gai Y, Peng H and Li J 2009 Electronic properties of nonstoichiometric PbSe quantum dots from first principles *J. Phys. Chem.* C **113** 21506–11

[102] Lin Q *et al* 2017 Phase-transfer ligand exchange of lead chalcogenide quantum dots for direct deposition of thick, highly conductive films *J. Am. Chem. Soc.* **139** 6644–53

[103] Shankar H, Ghosh S and Kar P 2022 Boosting the stability of lead halide perovskite nanocrystals by metal–organic frameworks and their applications *J. Mater. Chem.* C **10** 11532–54

[104] Kirkwood N, Monchen J O V, Crisp R W, Grimaldi G, Bergstein H A C, du Fossé I, van der Stam W, Infante I and Houtepen A J 2018 Finding and fixing traps in II–VI and III–V colloidal quantum dots: the importance of Z-type ligand passivation *J. Am. Chem. Soc.* **140** 15712–23

[105] Zhang F, Huang S, Wang P, Chen X, Zhao S, Dong Y and Zhong H 2017 Colloidal synthesis of air-stable $CH_3NH_3PbI_3$ quantum dots by gaining chemical insight into the solvent effects *Chem. Mater.* **29** 3793–9

[106] Sun H, Li Z, Kong L, Wang B, Zhang C, Yuan Q, Huang S, Liu Y and Li L 2018 Enhancing the stability of $CsPbBr_3$ nanocrystals by sequential surface adsorption of S_2^- and metal ions *Chem. Commun.* **54** 9345–8

[107] Page R C *et al* 2015 Near-unity quantum yields from chloride treated CdTe colloidal quantum dots *Small* **11** 1548–54

[108] Houtepen A J, Hens Z, Owen J S and Infante I 2017 On the origin of surface traps in colloidal II–VI semiconductor nanocrystals *Chem. Mater.* **29** 752–61

[109] Soosaimanickam A, Adl H P, Chirvony V, Rodríguez-Cantó P J, Martínez-Pastor J P and Abargues R 2021 Effect of alkali metal nitrate treatment on the optical properties of $CsPbBr_3$ nanocrystal films *Mater. Lett.* **305** 130835

[110] Wang Y-K *et al* 2021 All-inorganic quantum-dot LEDs based on a phase-stabilized α-$CsPbI_3$ perovskite *Angew. Chem., Int. Ed.* **60** 16164–70

[111] Ahmed G H, El-Demellawi J K, Yin J, Pan J, Velusamy D B, Hedhili M N, Alarousu E, Bakr O M, Alshareef H N and Mohammed O F 2018 Giant photoluminescence enhancement in $CsPbCl_3$ perovskite nanocrystals by simultaneous dual-surface passivation *ACS Energy Lett.* **3** 2301–7

[112] Hoang M T, Pannu A S, Yang Y, Madani S, Shaw P, Sonar P, Tesfamichael T and Wang H 2022 Surface treatment of inorganic $CsPbI_3$ nanocrystals with guanidinium iodide for efficient perovskite light-emitting diodes with high brightness *Nano-Micro Lett.* **14** 69

[113] Joo W-J *et al* 2020 Metasurface-driven OLED displays beyond 10,000 pixels per inch *Science* **370** 459–63

[114] Vasilopoulou M, Fakharuddin A, García de Arquer F P, Georgiadou D G, Kim H, Mohd Yusoff A R B, Gao F, Nazeeruddin M K, Bolink H J and Sargent E H 2021 Advances in solution-processed near-infrared light-emitting diodes *Nat. Photon.* **15** 656–69

[115] Reineke S, Lindner F, Schwartz G, Seidler N, Walzer K, Lüssem B and Leo K 2009 White organic light-emitting diodes with fluorescent tube efficiency *Nature* **459** 234–8

[116] Pradhan S, Di Stasio F, Bi Y, Gupta S, Christodoulou S, Stavrinadis A and Konstantatos G 2019 High-efficiency colloidal quantum dot infrared light-emitting diodes via engineering at the supra-nanocrystalline level *Nat. Nanotechnol.* **14** 72–79

[117] Utzat H *et al* 2019 Coherent single-photon emission from colloidal lead halide perovskite quantum dots *Science* **363** 1068–72

[118] Kagan C R, Lifshitz E, Sargent E H and Talapin D V 2016 Building devices from colloidal quantum dots *Science* **353** aac5523

[119] Kress S J P *et al* 2017 A customizable class of colloidal-quantum-dot metallic lasers and amplifiers *Sci. Adv.* **3** e1700688

[120] Bae W K, Brovelli S and Klimov V I 2013 Spectroscopic insights into the performance of quantum dot light-emitting diodes *MRS Bull.* **38** 721–30

[121] Zhang H, Feng Y and Chen S 2016 Improved efficiency and enhanced color quality of light-emitting diodes with quantum dot and organic hybrid tandem structure *ACS Appl. Mater. Interfaces* **8** 26982–8

[122] Yang J *et al* 2020 High-resolution patterning of colloidal quantum dots via non-destructive, light-driven ligand crosslinking *Nat. Commun.* **11** 2874

[123] Lim J, Park Y-S, Wu K, Yun H J and Klimov V I 2018 Droop-free colloidal quantum dot light-emitting diodes *Nano Lett.* **18** 6645–53

[124] Samarakoon C *et al* 2022 Optoelectronic system and device integration for quantum-dot light-emitting diode white lighting with computational design framework *Nat. Commun.* **13** 4189

[125] Jung S-M *et al* 2021 Modelling charge transport and electro-optical characteristics of quantum dot light-emitting diodes *npj Comput. Mater.* **7** 122

[126] Deng Y *et al* 2022 Solution-processed green and blue quantum-dot light-emitting diodes with eliminated charge leakage *Nat. Photon.* **16** 505–11

[127] Zhang W *et al* 2024 Stable and efficient pure blue quantum-dot LEDs enabled by inserting an anti-oxidation layer *Nat. Commun.* **15** 783

[128] Shen H *et al* 2019 Visible quantum dot light-emitting diodes with simultaneous high brightness and efficiency *Nat. Photon.* **13** 192–7

[129] Cheng Y, Wan H, Liang T, Liu C, Wu M, Hong H, Liu K and Shen H 2021 Continuously graded quantum dots:

synthesis, applications in quantum dot light-emitting diodes, and perspectives *J. Phys. Chem. Lett.* **12** 5967–78
[130] Huang Y-M, Singh K J, Liu A-C, Lin C-C, Chen Z, Wang K, Lin Y, Liu Z, Wu T and Kuo H-C 2020 Advances in quantum-dot-based displays *Nanomaterials* **10** 1327
[131] Ma L, Han B, Zhang F, Xu L, Fang T, Wang S and Song J 2021 Recent progress on defect modulation for highly efficient metal halide perovskite light-emitting diodes *Appl. Mater. Today* **22** 100946
[132] Linkov P, Samokhvalov P, Vokhmintsev K, Zvaigzne M, Krivenkov V A and Nabiev I 2019 Optical properties of quantum dots with a core–multishell structure *JETP Lett.* **109** 112–5
[133] Bajwa P 2016 *Role of the Inner Shell Architecture on the Various Blinking States and Decay Dynamics of Core-Shell and Core-Multishell Quantum Dots* (University of Arkansas)
[134] Zhang Y, Kaji N, Tokeshi M and Baba Y 2007 Nanobiotechnology: quantum dots in bioimaging *Expert Rev. Proteomics* **4** 565–72
[135] Zhang B-B *et al* 2019 General mild reaction creates highly luminescent organic-ligand-lacking halide perovskite nanocrystals for efficient light-emitting diodes *J. Am. Chem. Soc.* **141** 15423–32
[136] Lee J-S, Kovalenko M V, Huang J, Chung D S and Talapin D V 2011 Band-like transport, high electron mobility and high photoconductivity in all-inorganic nanocrystal arrays *Nat. Nanotechnol.* **6** 348–52
[137] Yang J-N *et al* 2023 Pseudohalogen resurfaced $CsPbBr_3$ nanocrystals for bright, efficient, and stable green-light-emitting diodes *Nano Lett.* **23** 3385–93
[138] Lu M, Guo J, Lu P, Zhang L, Zhang Y, Dai Q, Hu Y, Colvin V L and Yu W W 2019 Ammonium thiocyanate-passivated $CsPbI_3$ perovskite nanocrystals for efficient red light-emitting diodes *J. Phys. Chem.* C **123** 22787–92
[139] Chen T, Ru X-C, Ma Z-Y, Feng L-Z, Song K-H, Ge J, Zhu B-S, Yang J-N and Yao H-B 2024 Tetrafluoroborate-passivated $CsPbBr_xCl_{3-x}$ nanocrystals for spectrally stable pure blue perovskite light-emitting diodes *ACS Appl. Nano Mater.* **7** 4474–80
[140] Wang Y-K *et al* 2022 *In situ* inorganic ligand replenishment enables bandgap stability in mixed-halide perovskite quantum dot solids *Adv. Mater.* **34** 2200854
[141] Zhu H, Tong G, Li J, Xu E, Tao X, Sheng Y, Tang J and Jiang Y 2022 Enriched-bromine surface state for stable sky-blue spectrum perovskite QLEDs with an EQE of 14.6% *Adv. Mater.* **34** 2205092
[142] Wu T *et al* 2020 High-performance perovskite light-emitting diode with enhanced operational stability using lithium halide passivation *Angew. Chem., Int. Ed.* **59** 4099–105
[143] Zhang W, Tan Y, Duan X, Zhao F, Liu H, Chen W, Liu P, Liu X, Wang K and Zhang Z 2022 High quantum yield blue InP/ZnS/ZnS quantum dots based on bromine passivation for efficient blue light-emitting diodes *Adv. Opt. Mater.* **10** 2200685
[144] Zheng Z, Ren Z, Xia W, Luo C, Li J, Ma W, Ji H, Shi H and Chen Y 2023 Bromide decorated eco-friendly ZnSeTe/ZnSe/ZnS quantum dots for efficient blue light-emitting diodes *Adv. Mater. Interfaces* **10** 2202241
[145] Feng Y, Li H, Zhu M, Gao Y, Cai Q, Lu G, Dai X, Ye Z and He H 2024 Nucleophilic reaction-enabled chloride modification on $CsPbI_3$ quantum dots for pure red light-emitting diodes with efficiency exceeding 26 % *Angew. Chem., Int. Ed.* **63** e202318777
[146] Zhang S, Yang L, Liu G, Zhang S, Shan Q and Zeng H 2023 Eco-friendly Zn–Ag–In–Ga–S quantum dots: amorphous indium sulfide passivated silver/sulfur vacancies achieving efficient red light-emitting diodes *ACS Appl. Mater. Interfaces* **15** 50254–64
[147] Cheng H, Wang W, Qiu H, Li F and Zheng Y 2024 Sulfate-passivated $CsPbI_3$ perovskite nanocrystals for efficient red light-emitting diodes *ACS Appl. Nano Mater.* **7** 6885–92
[148] Ru X-C, Yang J-N, Ge J, Feng L-Z, Wang J-J, Song K-H, Chen T, Yu Ma Z, Li L-Y and Yao H-B 2023 Robust sulfate anion passivation for efficient and spectrally stable pure-red $CsPbI_{3-x}Br_x$ nanocrystal light-emitting diodes *Adv. Opt. Mater.* **11** 2300606
[149] Yang F, Chen H, Zhang R, Liu X, Zhang W, Zhang J, Gao F and Wang L 2020 Efficient and spectrally stable blue perovskite light-emitting diodes based on potassium passivated nanocrystals *Adv. Funct. Mater.* **30** 1908760
[150] Shen Y *et al* 2021 Interfacial potassium-guided grain growth for efficient deep-blue perovskite light-emitting diodes *Adv. Funct. Mater.* **31** 2006736
[151] Yang J-N *et al* 2020 Potassium bromide surface passivation on $CsPbI_{3-x}Br_x$ nanocrystals for efficient and stable pure red perovskite light-emitting diodes *J. Am. Chem. Soc.* **142** 2956–67
[152] Chen H, Fan L, Zhang R, Liu W, Zhang Q, Guo R, Zhuang S and Wang L 2019 Sodium ion modifying *in situ* fabricated $CsPbBr_3$ nanoparticles for efficient perovskite light emitting diodes *Adv. Opt. Mater.* **7** 1900747
[153] Dong Y *et al* 2020 Bipolar-shell resurfacing for blue LEDs based on strongly confined perovskite quantum dots *Nat. Nanotechnol.* **15** 668–74
[154] Li N, Song L, Jia Y, Dong Y, Xie F, Wang L, Tao S and Zhao N 2020 Stabilizing perovskite light-emitting diodes by incorporation of binary Alkali cations *Adv. Mater.* **32** 1907786
[155] Zhao Y-Y, Liu Y-F, Bi Y-G, Li C-H, Wang Y-F, Li H-W, Zhang Q-W, Lv C and Wu Y-Q 2023 Improved performance of $CsPbBr_3$ light-emitting diodes based on zinc bromide passivated quantum dots *Org. Electron.* **116** 106775
[156] Chen Z, Zhou B, Yuan J, Tang N, Lian L, Qin L, Zhu L, Zhang J, Chen R and Zang J 2021 Cu_2^+-doped $CsPbI_3$ nanocrystals with enhanced stability for light-emitting diodes *J. Phys. Chem. Lett.* **12** 3038–45
[157] Chen Q, Cao S, Xing K, Ning M, Zeng R, Wang Y and Zhao J 2021 Mg_2^+-assisted passivation of defects in $CsPbI_3$ perovskite nanocrystals for high-efficiency photoluminescence *J. Phys. Chem. Lett.* **12** 11090–7
[158] Zhou X, Zhang J, Tong X, Sun Y, Zhang H, Min Y and Qian Y 2022 Near-unity quantum yield and superior stable indium-doped $CsPbBr_xI_{3-x}$ perovskite quantum dots for pure red light-emitting diodes *Adv. Opt. Mater.* **10** 2101517
[159] Zhu R, Luo Z, Chen H, Dong Y and Wu S-T 2015 Realizing Rec. 2020 color gamut with quantum dot displays *Opt. Express* **23** 23680–93
[160] Masaoka K and Nishida Y 2015 Metric of color-space coverage for wide-gamut displays *Opt. Express* **23** 7802–8
[161] Cho H *et al* 2015 Overcoming the electroluminescence efficiency limitations of perovskite light-emitting diodes *Science* **350** 1222–5
[162] Cheng L-P *et al* 2019 Efficient $CsPbBr_3$ perovskite light-emitting diodes enabled by synergetic morphology control *Adv. Opt. Mater.* **7** 1801534
[163] Shi Y *et al* 2018 A strategy for architecture design of crystalline perovskite light-emitting diodes with high performance *Adv. Mater.* **30** 1800251
[164] Dai X, Zhang Z, Jin Y, Niu Y, Cao H, Liang X, Chen L, Wang J and Peng X 2014 Solution-processed, high-performance light-emitting diodes based on quantum dots *Nature* **515** 96–99

[165] Yang Y, Zheng Y, Cao W, Titov A, Hyvonen J, Manders J R, Xue J, Holloway P H and Qian L 2015 High-efficiency light-emitting devices based on quantum dots with tailored nanostructures *Nat. Photon.* **9** 259–66

[166] Kim S-K, Yang H and Kim Y-S 2019 Control of carrier injection and transport in quantum dot light emitting diodes (QLEDs) via modulating Schottky injection barrier and carrier mobility *J. Appl. Phys.* **126** 18

[167] Yang S, Hoang M-S and Chen H-S 2023 Enhanced carrier mobility by doping NaCl in a hole-transport layer for electroluminescent quantum dots light-emitting diodes *ACS Appl. Nano Mater.* **6** 20367–74

[168] Zhang X, Wang S, Li D, Wang J and Liu H 2023 Synergistic regulation of hole and electron transport layers for efficient injection balance in deep blue quantum dot light-emitting diodes *ACS Mater. Lett.* **5** 3184–91

[169] Davidson-Hall T and Aziz H 2020 Significant enhancement in quantum dot light-emitting device stability via a cascading hole transport layer *ACS Appl. Mater. Interfaces* **12** 16782–91

[170] Kim D H, An H J, Choi I Y and Myoung J-M 2022 High-performance pure-red light-emitting diodes based on $CsPbBr_xI_{3-x}$–multi-ligands–KBr composite films *Chem. Eng. J.* **429** 132375

[171] Song J, Fang T, Li J, Xu L, Zhang F, Han B, Shan Q and Zeng H 2018 Organic–inorganic hybrid passivation enables perovskite QLEDs with an EQE of 16.48% *Adv. Mater.* **30** 1805409

[172] Zhou W, Shen Y, Cao L-X, Lu Y, Tang Y-Y, Zhang K, Ren H, Xie F-M, Li Y-Q and Tang J-X 2023 Manipulating ionic behavior with bifunctional additives for efficient sky-blue perovskite light-emitting diodes *Adv. Funct. Mater.* **33** 2301425

[173] Heimer T A, Bignozzi C A and Meyer G J 1993 Molecular level photovoltaics: the electrooptical properties of metal cyanide complexes anchored to titanium dioxide *J. Phys. Chem.* **97** 11987–94

[174] Lee J-H, Bae J-G, Kim M S, Heo J Y, Lee H J and Lee J H 2024 Effect of the interaction between transition metal redox center and cyanide ligand on structural evolution in Prussian white cathodes *ACS Nano* **18** 1995–2005

[175] Dronova M, Altenschmidt L, Bordage A, Brubach J-B, Verseils M, Balthazar G, Roy P and Bleuzen A 2024 Interactions between alkali cations and cyanide-bridged network in A_2Co_4 $[Fe(CN)_6]3.3$ Prussian blue analogues revealed by far-infrared spectroscopy *Mater. Adv.* **5** 3794–801

[176] Ott L S and Finke R G 2006 Nanocluster Formation and stabilization fundamental studies: investigating "Solvent-Only" stabilization En route to discovering stabilization by the traditionally weakly coordinating anion BF_4^- plus high dielectric constant solvents *Inorg. Chem.* **45** 8382–93

[177] Bour C, Monot J, Tang S, Guillot R, Farjon J and Gandon V 2014 Structure, stability, and catalytic activity of fluorine-bridged complexes IPr·$GaCl_2(\mu$-F)EF_{n-1} (EFn—= SbF_6^-, PF_6^-, or BF_4^-) *Organometallics* **33** 594–9

[178] Ba D, Gui Q, Liu W, Wang Z, Li Y and Liu J 2022 Robust cathode-ether electrolyte interphase on interfacial redox assembled fluorophosphate enabling high-rate and ultrastable sodium ion full cells *Nano Energy* **94** 106918

[179] Xie Y, Peng B, Bravić I, Yu Y, Dong Y, Liang R, Ou Q, Monserrat B and Zhang S 2020 Highly efficient blue-emitting $CsPbBr_3$ perovskite nanocrystals through neodymium doping *Adv. Sci.* **7** 2001698

[180] Firmino A D G, Figueira F, Tomé J P C, Paz F A A and Rocha J 2018 Metal–organic frameworks assembled from tetraphosphonic ligands and lanthanides *Coord. Chem. Rev.* **355** 133–49

[181] Zhang W, Li X, Peng C, Yang F, Lian L, Guo R, Zhang J and Wang L 2022 CsPb (Br/Cl) 3 perovskite nanocrystals with bright blue emission synergistically modified by calcium halide and ammonium ion *Nanomaterials* **12** 2026

[182] Bhawna K, Ghorui S, Alam A and Aslam M 2023 Advances in Synthesis and defect properties of halide perovskite nanocrystals: experimental and theoretical perspectives *Synthesis and Applications of Nanomaterials and Nanocomposites* (Springer) pp 3–37

[183] Muscarella L A and Ehrler B 2022 The influence of strain on phase stability in mixed-halide perovskites *Joule* **6** 2016–31

[184] Bai Y, Hao M, Ding S, Chen P and Wang L 2022 Surface chemistry engineering of perovskite quantum dots: strategies, applications, and perspectives *Adv. Mater.* **34** 2105958

[185] Xu F, Zhang M, Li Z, Yang X and Zhu R 2023 Challenges and perspectives toward future wide-bandgap mixed-halide perovskite photovoltaics *Adv. Energy Mater.* **13** 2203911

[186] Hahm D *et al* 2022 Direct patterning of colloidal quantum dots with adaptable dual-ligand surface *Nat. Nanotechnol.* **17** 952–8

[187] Park J-S *et al* 2016 Alternative patterning process for realization of large-area, full-color, active quantum dot display *Nano Lett.* **16** 6946–53

[188] Mei W, Zhang Z, Zhang A, Li D, Zhang X, Wang H, Chen Z, Li Y, Li X and Xu X 2020 High-resolution, full-color quantum dot light-emitting diode display fabricated via photolithography approach *Nano Res.* **13** 2485–91

[189] Kim G-H, Lee J, Lee J Y, Han J, Choi Y, Kang C J, Kim K-B, Lee W, Lim J and Cho S-Y 2021 High-resolution colloidal quantum dot film photolithography via atomic layer deposition of ZnO *ACS Appl. Mater. Interfaces* **13** 43075–84

[190] Bae J, Shin Y, Yoo H, Choi Y, Lim J, Jeon D, Kim I, Han M and Lee S 2022 Quantum dot-integrated GaN light-emitting diodes with resolution beyond the retinal limit *Nat. Commun.* **13** 1862

[191] Xie B, Zhao W, Luo X and Hu R 2023 Alignment engineering in thermal materials *Mater. Sci. Eng.* R **154** 100738

[192] Wang Y, Fedin I, Zhang H and Talapin D V 2017 Direct optical lithography of functional inorganic nanomaterials *Science* **357** 385–8

[193] Wang Y, Pan J-A, Wu H and Talapin D V 2019 Direct wavelength-selective optical and electron-beam lithography of functional inorganic nanomaterials *ACS Nano* **13** 13917–31

[194] Cho H, Pan J-A, Wu H, Lan X, Coropceanu I, Wang Y, Cho W, Hill E A, Anderson J S and Talapin D V 2020 Direct optical patterning of quantum dot light-emitting diodes via *in situ* ligand exchange *Adv. Mater.* **32** 2003805

[195] Pan J-A, Ondry J C and Talapin D V 2021 Direct optical lithography of $CsPbX_3$ nanocrystals via photoinduced ligand cleavage with postpatterning chemical modification and electronic coupling *Nano Lett.* **21** 7609–16

[196] Pan J-A, Wu H, Gomez A, Ondry J C, Portner J, Cho W, Hinkle A, Wang D and Talapin D V 2022 Ligand-free direct optical lithography of bare colloidal nanocrystals via photo-oxidation of surface ions with porosity control *ACS Nano* **16** 16067–76

[197] Pan J-A, Cho H, Coropceanu I, Wu H and Talapin D V 2023 Stimuli-responsive surface ligands for direct lithography of functional inorganic nanomaterials *Acc. Chem. Res.* **56** 2286–97

[198] Lee J, Ha J, Lee H, Cho H, Lee D C, Talapin D V and Cho H 2023 Direct optical lithography of colloidal InP-based quantum dots with ligand pair treatment *ACS Energy Lett.* **8** 4210–7